On Tunnelling In Two-Throat Warped Reheating

Peter Langfelder
Dept. Of Physics, University of Waterloo and Perimeter Institute
Waterloo, ON, Canada
plangfel@uwaterloo.ca

February 1, 2008

Abstract

We revisit the energy transfer necessary for the warped reheating scenario in a two-throat geometry. We study KK mode wavefunctions of the full two-throat system in the Randall–Sundrum (RS) approximation and find an interesting subtlety in the calculation of the KK mode tunnelling rate. While wavepacket tunnelling is suppressed unless the Standard Model throat is very long, wavefunctions of modes localized in different throats have a non-zero overlap and energy can be transferred between the throats by interactions between such KK modes. The corresponding decay rates are calculated and found to be faster than the tunnelling rates found in previously published works. However, it turns out that the imaginary parts of the mode frequencies, induced by the decay, slow the decay rates themselves down. The self-consistent decay rate turns out to be given by the plane wave tunnelling rate considered previously in the literature. We then discuss mechanisms that may enhance the energy transfer between the throats over the RS rates. In particular, we study models in which the warp factor changes in the UV region less abruptly than in the RS model, and find that it is easy to build phenomenological models in which the plane wave tunnelling rate, and hence the KK mode interaction rates, are enhanced compared to the standard RS setup.

Contents

1 Introduction

String theory provides several promising and in many ways natural avenues to address the origin and properties of inflation as well as the origin of hierarchies of energy scales. For example, when the 6-dimensional internal space consists of several (perhaps many) long throats joined by bulk [1], physical processes deep in a particular

throat will have their energies redshifted by an amount that depends on their position in the throat. In this manner one can obtain large hierarchies simply by cleverly choosing the internal geometry and positions of various physically important objects within it [1]: for example, placing the Standard Model on a stack of D branes deep inside a long throat can lead to a desired low SM energy scale [2, 3].

An interesting class of inflationary models in such a multi-throat background is driven by the potential energy of D3 and anti-D3 branes [4]. While the D3 branes are mobile, the anti-D3 branes are stuck at the bottom of one of the throats; during the "slow-roll" phase of inflation, the D3 branes move through the bulk and the appropriate throat(s) toward the anti-D3 branes [5, 6]. Once they get within about a string length, a tachyonic mode appears and the branes and antibranes annihilate, ending inflation. The annihilation is expected to produce a large number of very massive closed strings [7] that will quickly decay into the lowest string states [8], namely the (10-dimensional) graviton, the gauge fields and the dilaton, and their fermionic partners.

Typically the annihilating branes are assumed to be located in a moderately short throat, so inflation happens at the scale required by CMB observations, about 10^{14}–10^{15} GeV [9]. While the annihilation products have in principle enough energy to reheat our universe, the energy must first be transferred to our vicinity in the internal space, which usually means tunnelling through the bulk joining the throats. This issue received a good deal of attention recently [8, 9, 10, 11, 12, 13], with the general conclusion being that generically the tunnelling seems to be too slow, but can be made fast enough for certain specific choices of the parameters in the model.

Our aim is to make more precise several qualitative arguments and rough estimates used in the works cited above (the first attempt in this direction appeared in [8]). Further, we investigate various mechanisms that may enhance (or, in some cases, suppress) the rate of energy transfer between the annihilation (A) and the the Standard Model (SM) throats. Following [8, 9, 10], we will (mostly) work with two 5-dimensional AdS throats of constant (and equal) curvature separated by a UV brane (this setup can also be viewed as a two-fold copy of the Randall–Sundrum model [2], and we will occasionally refer to it as the doubled RS model).

We begin in Section 2 by reviewing the setup of [9, 14] that will be the background for our tunnelling and decay calculations. In Section 3 we consider, in full detail, the wavefunctions of KK modes in this model and compare them to the wavefunction of the 4-dimensional graviton (zero mode). We find that the KK mode wavefunctions are enhanced only within narrow "resonance" bands; the width (in energy) of these bands can also be interpreted as the tunnelling rate from the A throat into the SM one. In Section 3.3 we find that the narrow width is also responsible for the (perhaps surprising) fact that for tunnelling to actually happen, the SM throat must be much longer than the A throat.

Even if KK modes localized in the A throat do not tunnel, their wavefunctions have a small tail in the SM throat. Thus they can decay into KK modes localized in the SM throat. In Section 4 we study the corresponding decay rates. Our results indicate that the decay into KK modes is faster than the tunnelling rates calculated in [8, 9, 14] and can dominate even if the SM throat is not as long as would be required for tunnelling. However, it turns out that the fast decay rates are not physical: in Section 5 we discuss modifications of the decay rate calculations due to different decay rates in the A and SM throats.[1] We find that having different decay rates in the two throats changes the shape of the wavefunction dramatically: the mode will penetrate the side on which it decays faster only to a certain distance that is inversely proportional to the decay rate. This implies that long throats cannot enhance decay rates indefinitely; in fact, it turns out that the self-consistent decay rate is limited by the plane wave tunnelling rate considered in [8, 9, 14]. We conclude that the plane wave tunnelling is realized, but only because the tunnelled particles decay in the SM throat fast enough.

Lest the reader thinks that this whole exercise simply re-derived a simple result in a complicated way, the calculation of the self-consistent decay rate allows us to check that the tunnelling and decay are not slowed down further by the effect of complex frequencies (this possibility was pointed out in [10]).

In Section 6 we look at a possible mechanism for energy transfer that arises during SM throat relaxation after inflation. Intuitively it can be understood as follows: as the length of the SM throat increases, the spectrum

[1] We were motivated by [10] who argue that differing decay rates can lead to a significant suppression of tunnelling.

of masses of its KK modes shifts down, while the A throat KK mode masses remain unchanged. When an SM throat eigenvalue approaches an A throat eigenvalue, instead of crossing they "repel" each other[2]: what was a KK mode localized in the A throat becomes a mode localized in the SM throat and vice-versa. Thus, KK modes and their energy could be "sucked" out of the A throat and into the SM throat where they could decay before another level repulsion would push them back. Unfortunately it turns out that the presence of an imaginary part of the mode mass (due to the decay) allows modes to avoid each other in the complex plane, and the mode switching between throats will not take place.

In Section 7 we consider models that exhibit enhanced tunnelling rates, either due to resonant effects (such as the ones mentioned in [12, 13]) or because the shape of the potential barrier separating the throats is modified (and the barrier is lowered). The basic idea is to modify the throats near their top, where the effective potential barrier is largest. Examples we look at include two throats with different curvature radii, resonant tunnelling through the gravity box of [15], and a toy 5-dimensional model representing two throats joined smoothly in the bulk, in which the curvature is changing stepwise due to the presence of additional 3-branes.[3] We show in Section 7 that low curvature in the central bulk region of the geometry can, under fairly general assumptions, lead to a drastic enhancement of tunnelling rates for the low-lying KK modes. We end in Section 8 with discussion and conclusions.

2 Review: Model of a two-throat compactification

We start by reviewing the 5-dimensional model of [9, 14]. We first summarize the background geometry, then concentrate on the fluctuations of the 5-dimensional metric as in [15].

2.1 Background

We start with an infinite Standard Model (SM) throat and in later sections generalize our analysis to the case of a finite SM throat[4]. Thus, our setup is Einstein's gravity in 5 dimensions parametrized by (x^μ, z) with $\mu = 0, .., 3$, with a "Planck" (UV) 3-brane embedded at $z = 0$ and an "annihilation" (A) brane embedded at $z = -z_A < 0$. The Planck and A branes have tensions V and $-V$ ($V > 0$), respectively. The coordinate z thus runs from $-z_A$ to ∞. To simplify notation, however, we will use positive z values on both sides of the UV brane and will distinguish them by superscripts A (annihilation side) and S (Standard Model side). The action is

$$S = \int \mathrm{d}^4x dz \sqrt{-g} \left(2M_5^3 R - \Lambda\right) - \int d^4x \sqrt{-g_4(z=0)} V + \int d^4x \sqrt{-g_4(z=z_A)} V. \tag{2.1}$$

At $z = z_A$ we impose, for the mode analysis, Z_2 boundary conditions on both the background *and* the fluctuations. In Section 7 we discuss the appropriate boundary conditions for the tunnelling calculation.

The background consists of AdS bulk with metric

$$ds^2 = \sigma^2(z)(dx^2 + dz^2), \tag{2.2}$$

with the warp factor $\sigma(z)$ given by

$$\sigma(z) = \frac{1}{1 + k|z|}, \tag{2.3}$$

[2]This is known as level repulsion in standard Quantum Mechanics

[3]Our term "3-branes" in this sense simply means domain walls with arbitrarily chosen tension; they are not supposed to represent string theory D3-branes.

[4]According to a conjecture of [11], during inflation the SM throat warping cannot be stronger than the square of the A throat warping; it is assumed that after inflation ends the SM throat will settle into its "vacuum" (long) states, though this process may not be finished at the time relevant for KK mode tunnelling and decay.

and the curvature scale k (equivalently, the radius of curvature $L \equiv 1/k$) is determined by the cosmological constant $\Lambda > 0$ as

$$k^2 = \frac{-\Lambda}{24M_5^3}. \tag{2.4}$$

As is well-known [2], to get flat branes localized at definite points in the z direction, their tension V must be tuned to

$$V = \pm 24M_5^3 k\,, \tag{2.5}$$

where the plus and minus signs apply to the Planck and inflating branes, respectively. An extension of this formalism to the case where the curvatures on both sides of the brane are not the same is discussed in Section 7.1.

2.2 Fluctuations

We would like to study linearized fluctuations of the metric (2.2) along the lines of [15]. We restrict ourselves to the metric fluctuations in the directions parallel to the branes and parametrize the full metric as

$$ds^2 = \sigma^2 \left[(\eta_{\mu\nu} + \widetilde{h}_{\mu\nu}) dx^\mu dx^\nu + dz^2 \right], \tag{2.6}$$

with the fluctuations $h_{\mu\nu} = \sigma^2 \widetilde{h}_{\mu\nu}$ satisfying the 4-dimensional transverse–traceless gauge conditions. Setting

$$h_{\mu\nu} = e^{ipx} \sigma^{1/2} \psi_m(z) \epsilon_{\mu\nu}, \tag{2.7}$$

with $m^2 = -p^2$ being the four-dimensional mass of the fluctuations, the linearized Einstein equations for the metric fluctuations reduce to a one-dimensional problem

$$\left[-\frac{1}{2}\partial_z^2 + V(z) \right] \psi_m(z) = \frac{1}{2} m^2 \psi_m(z), \tag{2.8}$$

with the potential $V(z)$ given by

$$V(z) = \frac{15k^2}{8(k|z|+1)^2} - \frac{3k\sigma(z)}{2} \left(\delta(z) - \delta(z - z_A) \right). \tag{2.9}$$

The solution of (2.8) away from the branes is

$$\psi_m(z) = N_m \, (m\tilde{z})^{1/2} \left[Y_2(m\tilde{z}) + Q_m J_2(m\tilde{z}) \right], \tag{2.10}$$

where we have introduced

$$\tilde{z} \equiv z + \frac{1}{k} \tag{2.11}$$

to make the notation more compact.

We now take ψ_m to be of the general form (2.10), with coefficients N_m^S, Q_m^S and N_m^A, Q_m^A on the SM and A sides of the Planck brane, respectively. The coefficient Q_m^A will be determined by the jump condition coming from (2.8) at the A brane, while Q_m^S and the ratio N_m^S/N_m^A will be determined by the jump condition and continuity at the Planck brane.

The following relation, derived using standard Bessel function identities and valid away from the branes, will be useful:

$$\frac{\partial_z \psi_m(z)}{\psi_m(z)} = -\frac{3k}{2}\sigma(z) + m \frac{Y_1(m\tilde{z}) + Q_m J_1(m\tilde{z})}{Y_2(m\tilde{z}) + Q_m J_2(m\tilde{z})}. \tag{2.12}$$

Equation (2.8) and the Z_2 conditions imposed on the fluctuations $h_{\mu\nu}$ at the A brane lead to

$$\partial_z \psi_m(z \to z_A^-) = \frac{3k}{2} \sigma(z_A) \psi_m(z_A), \tag{2.13}$$

giving

$$Q_m^A = -\frac{Y_1(m\tilde{z}_A)}{J_1(m\tilde{z}_A)}. \tag{2.14}$$

Similarly, (2.8) at the Planck brane implies

$$-\frac{1}{2}\left(\partial_z\psi_m(0^+) - \partial_z\psi_m(0^-)\right) = \frac{3k}{2}\psi_m(0) \tag{2.15}$$

leading to

$$Q_m^S = -\frac{Y_1(m/k)\left[Y_2(m/k) + Q_m^A J_2(m/k)\right] + Y_2(m/k)\left[Y_1(m/k) + Q_m^A J_1(m/k)\right]}{J_2(m/k)\left[Y_1(m/k) + Q_m^A J_1(m/k)\right] + J_1(m/k)\left[Y_2(m/k) + Q_m^A J_2(m/k)\right]}. \tag{2.16}$$

Since the SM side is semi-infinite, we have a continuum of plane-wave normalizable modes with normalization constants given by [15]

$$N_m^S = \sqrt{\frac{1}{1 + (Q_m^S)^2}}. \tag{2.17}$$

Imposing continuity of ψ_m at $z = 0$ implies

$$N_m^A = N_m^S \frac{Y_2(m/k) + Q_m^S J_2(m/k)}{Y_2(m/k) + Q_m^A J_2(m/k)}. \tag{2.18}$$

2.3 Energy and curvature scales

Before proceeding with our calculations, we should understand the physical scales in the problem. In the RS scenario that serves as our toy model, we have several mass and length scales: the 5-dimensional Planck scale M_5, an independent scale k that sets the curvature radius of the AdS space and the tension of the branes, the length z_A of the A throat and an (apriori independent) scale M_A of the brane physics that produces the KK modes which are, in the warped reheating scenario, responsible for the transfer of energy to the SM side.

If our setup is to serve as a model of string theory compactifications, the parameters of our model must be matched to the appropriate scales in string compactifications. Hence we would like to take k to be somewhat below the strings scale M_s

$$k = \frac{M_s}{\gamma g_s^{1/4}} \tag{2.19}$$

with γ a numerical factor of order say 10 that roughly corresponds to the compactification radius of the internal manifold, and g_s the string coupling. Parametrized this way, the factor γ is related [8, 10] to the flux quantum numbers of the Klebanov–Tseytlin throat [17, 16] as

$$\gamma \sim (MK)^{1/4}. \tag{2.20}$$

The bare tension of the branes ($D3$ branes in string theory) is $\sim M_s^4/g_s$, with $g_s < 1$. The brane scale M_A would be given by the tension of the annihilating branes times the warp factor at the position of the annihilating branes,

$$\begin{aligned} M_A &= \frac{M_s}{g_s^{1/4}}\sigma_A \\ &= \frac{\gamma}{g_s^{1/4}} k\sigma_A \\ &\approx \gamma\frac{1}{z_A}, \end{aligned} \tag{2.21}$$

where we have denoted $\sigma_A \equiv \sigma(z_A)$. Thus, the effective mass scale on the A brane is somewhat (an order of magnitude, say) larger than $1/z_A$. The 4- and 5-dimensional Planck scales M_4, M_5 are related to the string mass M_s as

$$M_4^2 k = M_5^3 \sim M_s^3 g_s^{-3/4} \gamma^5 \,, \tag{2.22}$$

where we have assumed that the compactification volume of the internal 5 dimensions is $V_5 \sim k^{-5}$. Expressed in terms of the string compactification parameters, the ratio k/M_5 is

$$\frac{k}{M_5} \sim \gamma^{-8/3} \,. \tag{2.23}$$

The inflation scale H is different from M_A [11], and in this setup is

$$\begin{aligned} H &\sim \frac{1}{\gamma^3} M_4 \sigma_A^2 \\ &\sim \gamma k \sigma_A^2 \,, \end{aligned} \tag{2.24}$$

i.e., it differs from M_A by an extra factor of roughly[5] σ_A.

Assuming $H/M_4 \sim (10^{-8}\text{—}10^{-5})$ and the 4-dimensional Planck scale M_4 being not very different[6] from the string scale (and thus also from k) leads to the annihilation warp factor $\sigma_A \sim (10^{-3}\text{—}1)$ [11]. To exhibit issues peculiar to warped inflation, in the remainder of this work we will assume that σ_A is in the low end of that range.

3 Two throats full of modes

In this section we study quantitatively the wavefunctions of KK modes likely to be produced in the decay of closed string remnants of the brane annihilation. As opposed to [8, 10] who considered modes in each throat separately, we study the modes of the full two-throat system.

In Section 3.1 we revisit the enhancement of the KK mode wavefunctions compared to the graviton deep in the A throat. Most of our conclusions agree with the ones that [8, 9, 10] arrived at. The calculations are quite technical, so we relegate the details to Appendix A and provide only a summary in the main text. We find that most of the modes of the full two-throat system are suppressed at the A brane (compared to the graviton zero mode), even when their masses are of order of $1/z_A$; only modes that fall within narrow "resonance peaks" of width

$$\delta m \sim m^5/k^4 \tag{3.1}$$

have their wavefunctions enhanced. These narrow peaks correspond to the discrete spectrum of modes of the A throat when the latter is viewed as a system on its own.

The mode analysis allows us to exhibit tunnelling between the throats as a wavepacket decoherence effect in the combined system, which we describe in Section 3.2. Wavepackets localized in the A throat will be composed predominantly of modes falling within the narrow resonance peak; hence the tunnelling rate Γ can be viewed as the rate at which the wavepacket decoheres and the destructive interference in the SM throat disappears. The rate is given precisely by the (energy) width of the wavepacket,

$$\Gamma = \delta m \sim \frac{m^5}{k^4} \,. \tag{3.2}$$

This expression is analogous to the (inverse of the) "throat interaction time scale" given in [10].

In Section 3.3 we consider modifications of the tunnelling rate that arise when one makes the SM throat finite, with coordinate length z_S. The spectrum will be quantized roughly in units of $1/z_S$ (for $z_S \gg z_A$). We find

[5] Derivation of (2.24) again assumes $V_5 \sim 1/k^5$.

[6] $M_4 = M_s \gamma^3/g_s$; with standard assumptions M_4 will be a few orders of magnitude larger than M_s

that for very long SM throats the results are, as expected, unchanged. On the other hand, when the SM throat becomes so short that the mode spacing $1/z_S$ becomes longer than the width δm of the resonant peaks (3.1), a mode localized in the A throat will remain localized there forever (at the linearized level; interactions can lead to decay of the mode). The surprising observation is that this suppression of tunnelling will occur when

$$z_S < z_A \frac{k^4}{m^4}\,, \tag{3.3}$$

Interestingly, [11] argue that during inflation, the SM throat cannot be longer than roughly $z_A k/m$ which is much shorter than the above bound; after inflation ends, the SM throat presumable gradually relaxes to its full length, but the tunnelling may still be suppressed at the time the KK modes decay.

We now turn to detailed calculations.

3.1 Deep down in the throat: KK modes vs. the graviton

In any model of inflation it is important that after inflation ends, the fraction of energy that ends up in gravitons be small. In brane inflation this means that production of gravitons from brane annihilation should be suppressed compared to other modes (in this case the KK modes) that can transfer the energy released by annihilation to Standard Model matter.

The results of [8] indicate that the flat-space production rates of gravitons and KK modes in the decay of highly excited closed strings [7] are roughly (up to a factor of order 1) the same. Hence, in the warped case, the relative production rates of KK modes and gravitons will be determined predominantly by the size of their respective wavefunctions. Thus, we should compare the wavefunctions of low-lying KK modes ($m \ll k$) to the wavefunction of the zero mode. The KK modes were analyzed in the previous section, while the zero mode, including its normalization, is

$$\psi_0 = \frac{\sqrt{k}}{(k\widetilde{z})^{3/2}}\,. \tag{3.4}$$

To quantify the relative magnitudes of the wavefunctions, we will study the ratio

$$R_\psi(m) \equiv \frac{\psi_m(z_A)}{\psi_0(z_A)}\,, \tag{3.5}$$

and its physically meaningful integral (since the KK modes have a continuous spectrum)

$$p(m) = \int_0^m dm' R_\psi^2(m')\,. \tag{3.6}$$

The function $p(m)$ can be interpreted as the ratio of probability densities to find a KK mode of mass $m' < m$ and to find a graviton at the A brane. If the couplings of such KK modes and the graviton to the closed string remnants of brane annihilation is similar, $p(m)$ will roughly represent the relative abundance of KK modes vs. gravitons in the products of decay of the closed strings. Phenomenology requires that $p(m)$ be large.

One can consider KK modes with masses in two regimes: the first one will encompass "very light" KK modes in the sense that $mz_A \ll 1$. The second, "intermediate", regime contains masses such that $mz_A \sim 1$ while $mk \ll 1$. In a full two-throat system we have a (semi-)continuum of modes in both regimes; on the other hand, an approximation with two separate, weakly coupled throats indicates that only a restricted subset of modes should be important in the A throat, namely the modes of the full system that approximate the modes of the A throat separated from the rest. This turns out to be the case.

Very light KK modes, $mz_A \ll 1$, are expected to be suppressed on the A side simply because the A throat is shorter than the SM throat (which we assume to be infinite here). The mass is so small that the volcano potential (2.9) at the inflating brane is already large enough to suppress the mode: For $kz_A \gg 1$ the potential

is $V(z_A) \sim 1/z_A^2$, so one would expect that for the KK masses $m < 1/z_A$ the corresponding mode would be suppressed on the inflating brane. Explicit calculations in Appendix A.1 bear this expectation out: we find

$$R_\psi^2 \approx \frac{m}{k^2} \tag{3.7}$$

and

$$p(m) \approx \frac{1}{2}\frac{m^2}{k^2} \ll 1\,. \tag{3.8}$$

Hence, production of such low-lying KK modes will be greatly suppressed compared to the production of gravitons.

The situation is more interesting in the intermediate regime $mz_A \sim 1$. In Appendix A.2 we find that for generic masses, the corresponding KK modes are still suppressed,

$$R_\psi^2 \sim \frac{m}{k^2}\,, \tag{3.9}$$

so

$$p(m) \sim \frac{m^2}{k^2} \sim \sigma_A^2\,. \tag{3.10}$$

Here the equality holds only up to factors of order 1, which we denote by the $\sim$ symbol. This suppression is counterintuitive: one would expect the Bessel functions entering the KK mode wavefunctions to begin approaching their asymptotic regime and hence be enhanced (in the integrated ratio $p(m)$) by a factor of roughly σ_A^{-2}. To resolve this discrepancy, it helps to look at the plot of R_ψ as a function of the mass m, Fig. 5(b). The plot shows that modes with "generic" mass are, in fact, suppressed as indicated above; however, the plot also shows narrow resonant spikes in which the ratio R_ψ is large. The width of the spikes is estimated in Appendix A and turns out to be given by the formula (3.1),

$$\delta m \sim m^5/k^4\,. \tag{3.11}$$

The contribution of the spikes to the integrated ratio $p(m)$ turns out to be large and in fact confirms the intuitive argument for the KK mode enhancement:

$$p(m)_{spike} \sim \sigma_A^{-2}\,. \tag{3.12}$$

This resonance phenomenon may seem surprising, but in fact it is to be expected in a system that is effectively composed of two weakly coupled potential wells. Those modes of the full system that have a small overlap with the "native" modes of the A throat (viewed as a separate system) will be suppressed there; the only modes of the full system that can be large are those that have a large overlap with the native modes of the A throat.

3.2 Tunnelling as a decoherence effect

Having modes of the full system allows us to exhibit the tunnelling of KK modes from the A throat to the SM one as a decoherence phenomenon: creation of a KK mode in the A throat is viewed as setting up a wave packet localized near the bottom of the A throat. As usual in quantum mechanics, to study the time evolution of the packet one can, *e.g.,* expand it into eigenmodes of the full system (whose time evolution is known precisely). The initial expansion into eigenmodes is quite special (*i.e.,* coherent), giving zero throughout most of the full system (namely in the SM throat). As the eigenmodes evolve with different frequencies, the evolution will destroy the coherence and the wavepacket's wavefunction will develop a nonzero generic amplitude in the SM throat, corresponding to the KK mode tunnelling out of the A throat. Let us call the decoherence time, *i.e.,* the time it takes the (initially highly correlated) expansion coefficients to become essentially random, t_{tun}. One can estimate t_{tun} as the inverse of the spread in frequency, $(\delta m)^{-1}$, of the initial wave packet, or the decoherence (tunnelling) rate Γ_{tun} as the spread itself. As we have argued in the previous subsection, the KK modes in the

A throat will be predominantly produced in the narrow bands around the peaks of R_ψ; the width of these peaks was estimated in (A.23) and we have

$$t_{tun}^{-1} = \Gamma_{tun} \sim \delta m \sim \frac{m^4}{k^4}\frac{1}{\widetilde{z}_A} \sim \frac{m^4}{k^4} m\,. \tag{3.13}$$

The same expression was derived in Section 3 of [8], and a similar one was given Section 5 of [10] as the "interaction time scale"; however, the authors of [10] assumed the UV scale to be the 4-dimensional Planck mass M_4; our calculation above (and the calculations of [14]) confirm that the relevant UV scale here is the curvature scale k which is expected to be somewhat smaller than M_4.

3.3 (Non-)Tunnelling into a finite SM throat

In deriving (3.13) we have assumed that the SM throat is infinite, even though in reality it will be long but finite; we will now clarify how long it must be to be for our preceding calculations to apply (inasmuch as our results agree with the ones in [8, 10], this restriction applies to those works as well). Hence, in this section we will assume the SM throat is cut off at $z = z_S > z_A$, with the $>$ sign meaning at least 1 order of magnitude.

If the SM throat is finite with length z_S, KK modes of the full system will be quantized roughly in units of $\delta_s m \sim 1/z_S$. One might think that simply having $z_S > z_A$ would mean that from the A throat point of view we a have a quasi-continuous spectrum, but this is not the case. The fastest way to see it is to consider the resonant spikes in R_ψ discussed in Section 3.1 and Appendix A.2: the width of these spikes is $\delta m \sim (m/k)^4 z_A^{-1} \ll z_A^{-1}$. In fact, if the spacing $\delta_s m$ is larger than the width of the spikes, it is likely that none of the modes present in the system will fall within the interval δm, indicating a suppression of tunnelling. This argument is a bit naive in that in addition to the $\delta_s m$ spaced modes (that one can consider to be native to the SM throat) there will be extra modes with spacing $\delta_A m \sim 1/z_A$ that are mostly localized in the A throat; however, precisely because these modes are localized in the A throat, wavepackets consisting mainly of such modes cannot tunnel.

To put some firm math behind the intuition we consider modes in the finite two-throat system explicitly. The boundary condition (2.14) now applies to the SM side as well (with the obvious modification),

$$Q_m^S = -\frac{Y_1(m\tilde{z}_S)}{J_1(m\tilde{z}_S)}\,. \tag{3.14}$$

Modes of the full system have masses m for which Q_m^A and Q_m^S satisfy (2.16).

The discrete spectrum of modes implies a change in normalization: just like the zero mode, the massive modes are now normalizable in the conventional sense,

$$\int dz\, \psi_m^2(z) = 1\,. \tag{3.15}$$

Fortunately, the normalization integrals for the wavefunctions given by (2.10) can be evaluated in a closed form. We list them here for future use and define a shorthand notation:

$$C_J(x) \equiv \int dx\, x J_2^2(x) = \frac{1}{2}x^2\left[J_2^2(x) - J_1(x)J_3(x)\right]\,, \tag{3.16}$$

$$C_Y(x) \equiv \int dx\, x Y_2^2(x) = \frac{1}{2}x^2\left[Y_2^2(x) - Y_1(x)Y_3(x)\right]\,, \tag{3.17}$$

$$C_{JY}(x) \equiv \int dx\, x Y_2(x)J_2(x) = \frac{1}{4}x^2\left[2J_2(x)Y_2(x) - J_1(x)Y_3(x) - Y_1(x)J_3(x)\right]\,. \tag{3.18}$$

To get oriented, let us first look at modes that are mostly localized in the SM throat (these are the equivalents of the "generic" modes discussed in Appendix A.2). Such modes have $Q_m^A \sim 1$ (*i.e.,* the Bessel functions entering (2.14) have generic values); this implies

$$Q_m^S \sim \frac{k^2}{m^2} \gg 1\,, \tag{3.19}$$

meaning that the masses of such modes lie near the zeros of $J_1(m\tilde{z}_S)$, confirming the intuition that the mass would be quantized in units of $1/z_S$. Since $Q^S_m \gg Q^A_m$, the normalization will be determined predominantly by $C_J(m\tilde{z}_S)$ and works out to be

$$N^S_m \sim \frac{m}{Q^S_m C_J(m\tilde{z}_S)} \sim \frac{m^2}{k^2\sqrt{z_S}}\,. \tag{3.20}$$

Continuity of ψ_m, Eq. (2.18), then gives

$$N^A_m \approx N^S_m\,, \tag{3.21}$$

and for the wavefunction itself we find

$$\psi^A_m(z_A) \sim \frac{m^2}{k^2\sqrt{z_S}}\,. \tag{3.22}$$

Comparing this with the zero mode wave function (3.4) we find

$$R^2_\psi(m) \sim \frac{m^4\tilde{z}^3_A}{k^2\tilde{z}_S} \sim \frac{m\,\delta_s m}{k^2}\,. \tag{3.23}$$

Summing over all modes whose $m \sim z_A$ we find the equivalent of (A.12),

$$p(m) = \sum_{m'\le m} R^2_\psi(m') \sim \frac{m^2}{k^2}\,. \tag{3.24}$$

(We have not explicitly considered the very light modes, but just as in the continuous case, their contribution scales the same with m/k.) This means that the generic (or SM throat) modes are small in the A throat. In the continuum case we found that most of the KK mode presence was due to a narrow range of modes that we called resonant. In the discrete case such modes occur when Q^S_m is (nearly) zero and large Q^A_m is large: $Q^S_m = 0$ implies, via (2.16),

$$Q^A_m \sim \frac{k^2}{m^2} \gg 1\,. \tag{3.25}$$

In this case the biggest contribution to the normalization integrals can come either from $C_Y(\tilde{z}_S) \sim m\tilde{z}_S$ or from $C_J(\tilde{z}_A) \sim m\tilde{z}_A k^4/m^4$, depending on the relative size of z_A, z_S and $1/k$.

If the SM side dominates, namely for

$$z_S > z_A\frac{k^4}{m^4}\,, \tag{3.26}$$

the mode will be mostly localized on the SM side despite being large in the A throat, simply because the SM throat is so long that the probability of finding the particle in it is close to 1. This is the case that closely approximates the continuum setup: the resonant KK modes are large in the A throat, yet if a wave packet localized in the A throat is formed from them, it will tunnel to the SM throat as discussed in Section 3.2. Eq. (3.26) confirms the intuitive arguments given at the start of this section: precisely when the former is satisfied, the spacing of the SM throat modes is fine enough that some will fit into each resonant spike.

On the other hand, if the A side dominates, namely for

$$z_S < z_A\frac{k^4}{m^4}\,, \tag{3.27}$$

we find a surprising result: the KK modes that are large in the A throat have a very small probability of being detected in the SM throat, and if a wave packet of such modes is formed in the A throat, it will generically remain there[7]; only a small part of order $z_S m^4/(z_A k^4) < 1$ of these KK modes will tunnel. Note that this can

[7]It may be possible to form a coherent wave packet that will appear very briefly in the SM throat, but it will decohere quickly and the particle(s) will reappear in the A throat again.

be the case even if the A throat is much shorter: *e.g.,* if $m \sim 1/z_A \sim 10^{-3}k$, the A throat can be almost 12 orders of magnitude shorter!

The preceding arguments provide a further constraint on the relative length of the throats: since the modes relevant to tunnelling have masses of order $1/z_A$, Eq. (3.26) implies

$$z_S > \sigma_A^4 z_A \,. \tag{3.28}$$

Written in terms of warp factors, we have a constraint on the Standard Model warp factor $\sigma_S \equiv \sigma(z_S)$ that reads

$$\sigma_S < \sigma_A^5 \,. \tag{3.29}$$

This is a stringent constraint; in fact, [11] suggests that during and shortly after inflation, the warp factor of the SM throat is no less than the square of the A warp factor,

$$\sigma_S \gtrsim \sigma_A^2 \,, \tag{3.30}$$

and hence the inequality (3.29) would not be satisfied.[8]

In Appendix B we show that a condition similar to (3.26) can be derived in a toy model of a δ-function potential barrier separating two finite flat boxes. A natural question to ask is what is the physical interpretation of the factor m^4/k^4 relating the two throat lengths in (3.26) and its analog in the δ-barrier case. We propose that, in general, tunnelling will occur only if the level spacing of the target side is finer than the level spacing on the source side multiplied by what one may call "plane wave tunnelling probability" P,

$$(\delta m)_{target} < P(\delta m)_{source} \,. \tag{3.31}$$

The tunnelling probability P is the "usual textbook" probability of a particle that starts as a plane wave far from the barrier on the source side to emerge as the corresponding plane wave on the target side. For the Randall–Sundrum model P was calculated by [14] and found to be $P \sim m^4/k^4$; we show in Appendix B that (3.31) also applies to the δ potential barrier.

In retrospect, at least naively, this looks like an obvious statement: the size of the wavefunction squared, *i.e.,* the probability density, in the target well is suppressed by the tunnelling rate with respect to the probability density in the source well; hence their lengths must differ by the corresponding factor for the probabilities (which are integrals of the densities) to be comparable. However, the statement uses the tunnelling rate of plane waves (which is independent of the lengths of the wells) to compare the tunnelling probabilities of wave packets made of standing waves in finite wells (and in finite wells the spectrum and tunnelling probabilities do depend on the lengths of the wells), so perhaps the result is not so obvious after all.

Incidentally, the above result, if true in general, would be applicable also to the multibrane setups considered in Section 7; the enhancement of the tunnelling rates of plane waves implies that the ratio of throat warp factors need not be as large as indicated in (3.29).

Before we end this section, a comment is in order about an apparent discrepancy with [8], whose authors claim that tunnelling rates are essentially (*i.e.,* up to factors of order 1) unaffected by making the SM throat short. The calculation in Appendix A of [8] appears to agree with ours above (although it is formulated in different terms), but their interpretation is incorrect in the sense that [8] split standing waves into in- and out-going parts and then regard the latter as independent, interpreting the outgoing component as representing a flux of tunnelled particles.

4 Energy transfer via decay without tunnelling

If the throat lengths are such that A throat KK modes remain localized in the A throat indefinitely, the said KK modes will decay via the nonlinear interactions present in the Einstein–Hilbert Lagrangian (and via the

[8] As we explain in Section 7.2, it is possible, if somewhat contrived, to relax (3.29) if the throats have different curvatures.

coupling of the 5-dimensional gravitational fluctuations to the SM brane fields). One might expect that for the lowest A throat KK mode the only decay channel would be pairwise annihilation into gravitons, but this is not so: the wavefunction of A throat KK modes has a small tail in the SM throat, and the tail actually causes a sizable decay rate into SM throat KK modes. In this section we study this decay rate and find that in general it appears to be faster than the plane wave tunnelling rate.

Before we dive into the calculations, however, a cautionary note is in oder. It is clear that the amplitude of the A throat KK wavefunction tail in the SM throat depends to a large degree on the potential shape in the UV region. For example, Ref. [13] found that tunnelling out of a full AdS_5 throat into the bulk is suppressed compared to the analogous quantity in the RS model; this suppression can be viewed as due to a modification of the effective potential entering the Schrödinger Equation (2.8). While the Randall–Sundrum geometry is a good approximation deep in the throat, the region near the UV brane will presumably look very different in (a dimensional reduction of) a full string compactification. With this possible loophole in mind, let us proceed with the actual calculation of the decay rates.

We start by quantifying the interaction strengths, following [9]. The 5-dimensional Einstein–Hilbert Lagrangian $M_5^3\sqrt{\widetilde{g}}R$ gives rise to an infinite series of interactions of the (canonically normalized) fluctuations h of the metric $\widetilde{g}$ around its background value g ($\widetilde{g} = g + M_5^{3/2}h$). Schematically they are of the form

$$\mathcal{L}_n \sim \frac{1}{M_5^{3n/2-3}} \int \sqrt{g}\, \nabla^2 \left[\left(g^{-1}\right)^{n+1} h^n \right] \tag{4.1}$$

where the derivatives can act both on the background metric and the fluctuations. We will only be interested in the powers of the warp factor and will neglect all order 1 coefficients (in particular, we will not attempt to keep track of the factors arising from various possibilities of contracting the indices in (4.1)).

A z-derivative acting on g^{-1} will give $k\sigma g^{-1}$ (derivatives in the x^μ directions are zero). A z-derivative acting on h will produce several terms that can be roughly characterized as being either of the form $k\sigma h$ or mh, where m is the mass of the KK mode. Derivatives of h in the x^μ directions will simply multiply the wave function by the corresponding momentum. Hence the interaction (4.1) leads to the following 3 basic types of terms,

$$\mathcal{L}_n \sim \frac{1}{M_5^{3n/2-3}} \int \sqrt{g}\, \left(g^{-1}\right)^{n+1} h^n \left\{ (p\cdot p, mm), mk\sigma, (k\sigma)^2 \right\} \tag{4.2}$$

(We consider the $p\cdot p, mm$ terms to be of the same type; note that the $p\cdot p$ and mm symbols should not be taken at face value; they could mean, *e.g.,* $p_1\cdot p_2$, $m_1 m_2$ if the derivatives act on different KK modes.) The terms differ by their z dependence and dependence on momenta.

To obtain an effective 4-dimensional interpretation, we perform the integral over z in (4.2); the results will be an effective 4-dimensional Lagrangian. We will treat all terms in (4.2) together; denote the power of $k\sigma$ by α (so $\alpha = 0, 1, 2$); then we can summarize (4.2) as

$$\mathcal{L}_n \sim \frac{1}{M_5^{3n/2-3}} \int d^4x dz\, \sqrt{g}\, \left(g^{-1}\right)^{n+1} h_1 \ldots h_n w_{(\alpha)} k^\alpha \sigma^\alpha \tag{4.3}$$

where $w_{(0)}$ is a combination of mm and $p\cdot p$, $w_{(1)} = km$ and $w_{(2)} = k^2$.

We recall from Section 2.2 that the z-dependence of the graviton fluctuations h is given by the KK mode wave function and the appropriate prefactor (we neglect the Lorentz tensor structure),

$$h(x,z) = \sigma^{1/2}(z)\psi(z)\phi(x) \tag{4.4}$$

where $\phi(x)$ is the 4-dimensional wavefunction that is usually taken to be simply $\exp(ipx)$. The n-point couplings can then be written concisely as

$$\mathcal{L}_n = \int d^4x\, \zeta_n \phi_1(x)\phi_2(x)\phi_3(x)\,, \tag{4.5}$$

where the "coupling constant" ζ_n (which in fact can contain factors of momenta) is the overlap integral along the z coordinate,

$$\zeta_n \sim \frac{1}{M_5^{3n/2-3}} \int dz \, \sqrt{g} \left(g^{-1}\right)^{n+1} \sigma^{n/2} w_{(\alpha)} k^\alpha \sigma^\alpha \psi_1(z) \dots \psi_n(z) \,. \tag{4.6}$$

Amplitudes involving at least one graviton deserve a special consideration.[9] From the perspective of the effective 4-dimensional theory, (4-dimensional) general covariance requires that the graviton couple to the (4-dimensional) stress tensor, which must in this case be proportional to (4-dimensional) momenta; hence amplitudes that include a graviton can only be nonzero for $\alpha = 0$.

Evaluating the integral (4.6) is in principle (numerically) straightforward, but giving meaningful estimates is somewhat tedious because the dominant regions in the z-integrals depend on how many A throat KK modes, SM throat KK modes and gravitons enter the amplitude. Hence we will calculate the 3-point coupling (4.6) for 1 A throat KK mode with mass m_0 decaying into two SM throat KK modes with masses $m_{1,2}$.

In principle one could contemplate the coupling of the A throat KK mode to a graviton and an SM throat KK mode, or to two gravitons, but these couplings vanish: because of the graviton profile, a 3-point amplitude with $\alpha = 0$ and one graviton reduces to the scalar product (of the z-dependent wavefunctions) of the two remaining modes in the amplitude, which is zero whenever the two modes are different. (As noted earlier, the $\alpha \neq 0$ couplings involving gravitons must vanish by 4-dimensional general covariance.)

To perform the integration, we approximate the Bessel functions by their small argument approximations and asymptotic forms respectively, where appropriate. In the region of $\tilde{z} < 1/\sqrt{mk}$, which we will call the UV regime because it describes the region near the UV brane, the KK mode wavefunctions have the same functional form as the graviton wavefunction, but their normalization constants differ. For integrals that are mainly localized in the UV region we can neglect the oscillatory nature of the Bessel functions at large arguments; for integrals that receive large contributions from the asymptotic region, we will have to take the oscillations into account.

Near the UV brane in the A throat ($\tilde{z} < 1/\sqrt{mk}$), the wavefunction of an A throat KK mode behaves roughly as

$$\psi(z) \sim \sqrt{m} \sigma_A^{1/2} \sigma^{3/2}(z) \,, \tag{4.7}$$

while far from the UV brane ($m\widetilde{z} \sim 1$) it is

$$\psi(z) \sim \frac{1}{\sqrt{z_A}} = \sqrt{k} \sigma_A^{1/2} = \text{const} \,. \tag{4.8}$$

In the asymptotic region of the SM throat, the wavefunction of an A throat KK mode is

$$\psi(z) \sim \frac{1}{\sqrt{z_A}} \frac{m^2}{k^2} = \sqrt{k} \sigma_A^{1/2} \frac{m^2}{k^2} = \text{const} \,. \tag{4.9}$$

The wavefunction of an SM throat KK mode with mass m_i in the asymptotic region of the SM throat is

$$\psi(z) \sim \frac{1}{\sqrt{z_S}} = \sqrt{k} \sigma_S^{1/2} = \text{const} \,, \tag{4.10}$$

while in the A throat it is (here we assume $m_i \tilde{z}_A < 1$, so only the UV regime is realized)

$$\psi(z) \sim \frac{m_i^2}{k^2 \sqrt{z_S}} \sqrt{m_i \tilde{z}} \frac{1}{(m_i \tilde{z})^2} = \sqrt{m_i} \sigma_S^{1/2} \sigma^{3/2}(z) \,. \tag{4.11}$$

As we remarked above, the functional form of the KK modes in the UV regime and the graviton (given by (3.4)) is the same, only the normalization constants differ.

[9] We thank Henry Tye, Xingang Chen and Irina Mocioiu for corrections, discussions and suggestions on this point.

Under the approximations (4.7)–(4.11) the integrand in (4.3) will be a certain power of the warp factor $\sigma(z)$ (multiplied by various constant factors). If this power is negative or zero throughout most of the throat in which the integral is performed, the IR region of the throat will dominate the integral; however, if the power of $\sigma(z)$ is positive, the UV region will dominate.

The amplitude of interest here is the decay of an A throat KK mode. We will assume that we are dealing with the lowest-lying A throat mode; higher modes either decay into the lowest one or decay via the same channels as the one we are considering. The coupling to two SM throat KK modes is dominated by the IR region of the SM throat and is largest for the derivative coupling ($\alpha = 0$). The result is

$$\zeta^S_{A,2S} \sim \xi \frac{k^{1/2}}{M_5^{3/2}} w_0 \frac{m_0^2}{k^2} \sigma_A^{1/2} \sigma_S^{-3/2} \,. \tag{4.12}$$

In this case, the oscillatory nature of the wavefunctions cannot be neglected since the integrand is large in the asymptotic region. To remind us of the fact that the naive expression is an overestimate, we have inserted a factor of ξ in (4.12) to account for the extra suppression. The factor ξ can be roughly estimated as follows. The integrand is $\sim \sigma^{-3/2}(z)$ times a factor of type $\cos(m_i \tilde{z})$ for each wavefunction. The naive estimate of the integral, integrating z from 0 to z_S, would be $\sim \sigma_S^{-5/2}/k$. An improved estimate can be made by noting that $\prod \cos(m_i \tilde{z})$ can be written as a sum of sines and cosines of various sums and differences of the arguments $m_i \tilde{z}$. Hence a better approximation to the integrand would be $\sigma^{-3/2}(z) \cos(m\tilde{z})$; for a generic value of m the leading term in the integral would go as $\int dz \sigma^{-3/2}(z) \cos(m\tilde{z}) \sim \sigma_S^{-3/2}/m$. Comparing this result with the naive value fixes the correction factor to be $\xi \sim 1/(m\tilde{z}_S) \sim \sigma_S/\sigma_A$. We note that if the masses m_i entering the amplitude are tuned such that (say) $m_0 = m_1 + m_2$, the naive estimate is actually correct (as can be seen by taking a limit $m \to 0$ of the improved integral). However, this "resonance" cannot be used to enhance the coupling, because it happens precisely when the decay products are on the threshold and have zero available phase space. Including the correction factor gives an improved estimate of the $\zeta^S_{A,2S}$ coupling,

$$\zeta^S_{A,2S} \sim \frac{k^{1/2}}{M_5^{3/2}} w_0 \frac{m_0^2}{k^2} \sigma_A^{-1/2} \sigma_S^{-1/2} \,. \tag{4.13}$$

The couplings can be written in various forms using $m_0/k \sim \sigma_A$ and defining the Standard model mass scale $M_{SM} = M_5 \sigma_S$; the ratio k/M_5 (an independent parameter in the RS model) is in a string compactification determined by the compactification moduli.

To obtain decay rates from the above couplings, one must perform a sum over accessible final states. In Appendix C we perform the sums in detail; however, up to numerical factors, the correct results can be obtained by simply assuming that all momentum factors are of order m_0 and simply multiplying the resulting coupling (or decay rate) by the number of accessible modes, which in case of a decay into two KK modes it will be n_{KK}^2. For the decay into two SM throat KK modes, the coupling (4.12) and (C.10) give the decay rate

$$\Gamma_{A,2S} \sim k \left(\frac{k}{M_5} \right)^3 \sigma_A^8 \sigma_S^{-3} \,. \tag{4.14}$$

This rate is quite fast; in particular, by making the SM throat long enough, it could be made much faster than the plane wave tunnelling rate (3.13). However, in the next section we show that the actual decay rate is slower than (4.14).

5 Tunnelling is back: Effects of decay on KK mode wavefunctions

In the previous section we have found the decay rate (4.14) of an A throat KK mode in the SM throat. The A throat KK modes can also decay in the A throat itself by pairwise annihilation into gravitons; the rate of this process was estimated in [8] to be

$$\Gamma_{A,2g} \sim k \sigma_A^3 \,. \tag{5.1}$$

Generically, the throat lengths are expected to be such that $\Gamma_{A,2S} \gg \Gamma_{A,2g}$. In this section we would like to incorporate the effects of unequal decay rates into our treatment of the two-throat system.[10]

Let us first use intuitive arguments to show what we expect to find. Wavefunction decay can be modelled by the presence of a sink (an imaginary term in the potential). If the sink varies as a function of the spatial coordinate (in our case, z), the wavefunction will tend to decay at different rates in different regions. Such a process would increase its gradient energy too much; to counteract it, there will be a non-zero probability current from regions with a small sink to regions with a large sink. In the case of two throats with different (but constant within each throat) sinks we may expect that the throat with the smaller sink will act as a "reservoir" from which the probability density will slowly "seep" into the throat with the big sink. The seepage between throats is expected to be slow because of the presence of the potential barrier. In the throat with the big sink, we have a source (incoming current density) at the top of the throat while the sink is present throughout, so we would expect the wavefunction to be largest near the source and decrease as a function of the coordinate z along the throat. A toy model of such a situation for a δ-function barrier separating two square wells is presented in Appendix D; the model confirms the intuition outlined above.

An additional feature of the RS setup is that the decay rates, and hence also the sinks, depend on wavefunction overlaps; as we argued above, the wavefunction of the decaying mode will, in turn, depend on the decay rates. Thus a would-be large decay rate in the SM throat would mean that the overlap integrals are actually small, so the actual decay rate cannot be too fast. How fast is too fast? Physically, the decay rate in the SM throat cannot be faster than the rate at which probability density leaks from the A throat into the SM throat – the presence of the barrier here turns out to be the limiting factor in the decay rate. We show that in the presence of a large sink, the wavefunction in the SM throat actually becomes a (spatially decaying) outgoing wave, and the "leakage rate" becomes simply the plane wave tunnelling rate through the barrier.

We now describe detailed calculations supporting the intuitive arguments just given. We start by analyzing the wavefunctions of the KK modes in the presence of sinks and then give an improved calculation of the decay rate $\Gamma_{A,2S}$ from Section 4.

5.1 KK modes in the presence of sinks

The effect of decay of KK modes will be represented by an imaginary term iS in the potential $V(z)$ in the effective Schrödinger equation (2.8). We will take S to be constant in each throat, but the values S^A and S^S in the A and SM throats, respectively, will be different (this is a simplification of the real problem where the decay term varies smoothly with z; the advantage is that it has a simple analytic solution). The 5-dimensional graviton fluctuations still have the form (2.7), but now we allow the frequency $p^0 = \omega = m + i\Gamma$ to be complex. The effective Schrödinger equation is then

$$\left[-\frac{1}{2}\partial_z^2 + V(z) + iS\right]\psi_m(z) = \frac{1}{2}\omega^2\psi_m(z), \tag{5.2}$$

The solution is a generalization of (2.10): in the A and SM throats we have, respectively,

$$\psi_m(z) = \begin{cases} N_m^A\sqrt{k\tilde{z}}\left[Y_2(\lambda^A\tilde{z}) + Q_m^A J_2(\lambda^A\tilde{z})\right] & \text{for } z < 0\,, \\ N_m^S\sqrt{k\tilde{z}}\left[Y_2(\lambda^S\tilde{z}) + Q_m^S J_2(\lambda^S\tilde{z})\right] & \text{for } z > 0\,, \end{cases} \tag{5.3}$$

where the (complex) wavenumbers λ^A, λ^S are now different from the frequency (and from each other),

$$\lambda^A = \sqrt{\omega^2 - 2iS^A}\,, \tag{5.4}$$

$$\lambda^S = \sqrt{\omega^2 - 2iS^S}\,. \tag{5.5}$$

[10] We were motivated by Kofman and Yi [10] who suggest, by treating the two-throat system as two separate throats coupled weakly through the barrier, that differing decay rates (represented as differing imaginary parts in the modes' frequencies) will suppress tunnelling rates.

The matching conditions at the ends of the throats and at the UV brane are direct generalizations of the ones derived in Section 2.2: at the ends we have

$$Q_m^A = -\frac{Y_1(\lambda^A \tilde{z}_A)}{J_1(\lambda^A \tilde{z}_A)}, \tag{5.6}$$

$$Q_m^S = -\frac{Y_1(\lambda^S \tilde{z}_S)}{J_1(\lambda^S \tilde{z}_S)}, \tag{5.7}$$

while the jump and continuity conditions at the UV brane can be written as

$$\lambda^A \frac{Y_1(\lambda^A/k) + Q_m^A J_1(\lambda^A/k)}{Y_2(\lambda^A/k) + Q_m^A J_2(\lambda^A/k)} = -\lambda^S \frac{Y_1(\lambda^S/k) + Q_m^S J_1(\lambda^S/k)}{Y_2(\lambda^S/k) + Q_m^S J_2(\lambda^S/k)}, \tag{5.8}$$

$$N_m^A \left[Y_2(\lambda^A/k) + Q_m^A J_2(\lambda^A/k)\right] = N_m^S \left[Y_2(\lambda^S/k) + Q_m^S J_2(\lambda^S/k)\right]. \tag{5.9}$$

Let us see how the spectrum will look like. We will assume (based on the decay rate calculations) that the magnitude of the sink terms is much smaller than the curvature scale k^2 (indeed if they were not, bulk effects would invalidate our effective field theory analysis), though the sink terms can be comparable in magnitude to the typical (squared) KK mode mass scales $1/z_A^2$. Then we have $|\lambda^{A,S}| \ll k$ and we can apply the small-argument approximations (A.1) to the Bessel functions in the UV brane jump condition (5.8). Analogously to the sink-free case, the jump condition can only be satisfied when one of the Q_m coefficients is large. For definiteness let us look at the case when Q_m^A becomes large (such modes will again be the A throat modes). From (5.6) we find that $J_1(\lambda^A \tilde{z}_A)$ must be small, so $\lambda^A \tilde{z}_A$ must be near one of the roots of J_1, all of which are real. Hence λ^A will be (nearly) real (it will have a small imaginary part that is not important for us). This fixes λ_S to be

$$\lambda_S = \sqrt{(\lambda^A)^2 - 2i(S^S - S^A)}, \tag{5.10}$$

so $\lambda_S \equiv a + ib$ will have a substantial imaginary part b. The most important consequence of b is that in the asymptotic region of the SM throat the wavefunction $Y_2(\lambda^S \tilde{z}) + Q_m^S J_2(\lambda^S \tilde{z})$ drops off roughly as as $\exp(-b\tilde{z})$. This can be seen from the asymptotic form of the Bessel functions, namely

$$\sqrt{\pi x/2} J_\nu(x) \approx \cos(x - \nu\pi/2 - \pi/4), \tag{5.11}$$

$$\sqrt{\pi x/2} Y_\nu(x) \approx \sin(x - \nu\pi/2 - \pi/4). \tag{5.12}$$

Indeed, taking into account (5.7) we find

$$\psi(z) \approx \frac{2N_m^S}{\pi \cos(\lambda^S \tilde{z}_S)} \cos[\lambda^S(\tilde{z} - \tilde{z}_S)]$$
$$\sim N_m^S e^{-b\tilde{z}}. \tag{5.13}$$

Note that N_m^S remains finite in the limit $z_S \to \infty$.

This is an interesting result: it says that as long as the wavenumber λ_S^A has an imaginary part (which will be the case whenever $S^S \neq S^A$), the A throat KK modes will effectively penetrate the SM throat only to distance at most $z_p \sim 1/b$, no matter how long the throat is.

An important consequence of the finite penetration length, if it is shorter than the throat length z_S, is that it can lead to a substantial reduction of the overlap integrals (4.6) that are the coupling constants in the decay rates. We will now argue that the decay rate (4.14) is so fast that it implies a penetration length z_p much smaller than the length of the SM throat; hence, in a sense, the rate $\Gamma_{A,2S}$ is inconsistent and we must find a way of estimating the physically realized decay rate.

To obtain the penetration length z_p implied by the decay rate $\Gamma_{A,2S}$, we need to find the sink S^S that corresponds to $\Gamma_{A,2S}$. This problem is solved in Appendix E; the result is

$$b \sim \frac{S^S}{m} \sim k \frac{k^3}{M_5^3} \sigma_A^3 \sigma_S^{-2}, \tag{5.14}$$

so

$$\frac{z_S}{z_p} \sim \frac{k^3}{M_5^3}\sigma_A^3\sigma_S^{-3}\,. \tag{5.15}$$

Clearly, unless k/M_5 is extremely small, we find

$$z_p \ll z_S\,, \tag{5.16}$$

meaning, as we claimed above, that the penetration length is much shorter than the throat length and hence the physically realizable decay rate $\hat{\Gamma}_{A,2S}$ will be smaller than the result (4.14). We now estimate $\hat{\Gamma}_{A,2S}$.

5.2 Estimating the effective decay rate

We have an A throat mode that decays by interactions that are localized in the S throat. We argued above that its wavefunction will decay exponentially as a function of (coordinate) distance in the S-throat. The situation can be described as a reservoir of probability density in the A throat that slowly leaks into the S throat, where the probability density decays. Clearly, the probability decay rate cannot be faster than the rate of leakage; in fact, since the probability does not accumulate in the throat either, the decay and leakage rates must equal.

The leakage rate is given by the probability current

$$j_z \sim \frac{i}{m}\psi^* \overleftrightarrow{\partial}\, \psi \tag{5.17}$$

evaluated at the top of the throat. The current (5.17) will consist of two terms $j = j_1 + j_2$, with j_1 proportional to the imaginary part of the coefficient Q_m^S, while j_2 is proportional to the imaginary part of the wavenumber λ^S. Let us first look at j_1: using the asymptotic forms of the Bessel functions and $b\tilde{z}_S > 1$, we find

$$Q_m^S \approx -i \tag{5.18}$$

so the wavefunction in the SM throat is actually the outgoing Hankel function $H_2^+(\lambda\tilde{z})$! The parameter $\lambda\tilde{z}$ is complex, so the amplitude of the wavefunction decays exponentially, as we have shown in the previous section; near the top of the throat we find

$$j_1 \sim k\sigma_A^5 \sim m\sigma_A^4\,, \tag{5.19}$$

namely the rate at which plane waves tunnel between two infinite throats, considered in [14, 9, 8, 10]. The part j_2 of the current can be estimated as

$$j_2 \sim -j_1 \left|\frac{\text{Im}\,\{\lambda^S\}}{\text{Re}\,\lambda^S}\right|\,. \tag{5.20}$$

The negative sign is always present and means that the decay of the wavefunction further slows down the "leaking" of the probability density into the SM throat. An important question now is whether j_2 is comparable to j_1, that is whether the imaginary and real parts of the SM throat wavenumber λ^S are comparable. If it were so, the decay rate could be significantly suppressed even compared to the plane wave tunnelling rate (this possibility was also pointed out in [10]). As we argued earlier, the imaginary part of the wavenumber determines the penetration length z_p as $z_p^{-1} \sim \text{Im}\,\{\lambda^S\}$. In the following subsection we will estimate the latter and show that, at least in our approximation, the current j_2 is indeed negligible, so the effective decay rate roughly equals the plane wave tunnelling rate,

$$\hat{\Gamma}_{A,2S} \approx \Gamma_{tun} \sim m\sigma_A^4\,. \tag{5.21}$$

Thus, while the naive decay rate (4.14) is not the physical one because it is larger than the tunnelling rate, it does have a physical meaning: it is in turn small enough that current j_2 remains negligible compared to j_1.

5.3 Estimating the penetration length

We would like to calculate the penetration length $z_p \equiv b^{-1}$ of the A throat KK mode wavefunction into the SM throat self-consistently, at least within our approximations. The strategy is to calculate the decay rate $\hat{\Gamma}_{A,2S}(z_p)$ as a function of z_p, and equate it to the maximum physical rate (5.21).

The calculation will follow the same line as in Section 4, with the following modifications. First, we will assume that the decaying wavefunction, instead of decreasing exponentially with the characteristic length z_p, equals the naive wavefunction for $z < z_p$, and is zero for $z > z_p$; this means the overlap integral (4.6) will only extend to $z = z_p$. The wavefunctions entering the integral are still approximated by (4.9) and (4.10) and the result is (cf. (4.12))

$$\hat{\zeta}^S_{A,2S} \sim \hat{\xi} \frac{k^{1/2}}{M_5^{3/2}} w_0 \frac{m_0^2}{k^2} \sigma_A^{1/2} \sigma_S \sigma(z_p)^{-5/2} \,. \tag{5.22}$$

The correction factor $\hat{\xi}$ is now, in analogy with the discussion below (4.12), roughly

$$\hat{\xi} \sim \sigma_A^{-1} \sigma(z_p) \,, \tag{5.23}$$

so the improved coupling can be written as

$$\hat{\zeta}^S_{A,2S} \sim \frac{k^{1/2}}{M_5^{3/2}} w_0 \sigma_A^{3/2} \sigma_S \sigma(z_p)^{-3/2} \,. \tag{5.24}$$

Calculating the decay rate also involves summing over accessible final states. Since the wavefunction of the decaying mode only penetrates the SM throat to distance z_p, it will only couple (appreciably) to SM throat modes whose mass is large enough for them to not be suppressed for $z < z_p$, so we will only include modes of mass $m > 1/z_p$ in the sum over final states. Roughly speaking this means that the number of accessible final states changes from $z_S m_0$ to $z_p m_0$. Applying the results of Appendix C we find

$$\hat{\Gamma}_{A,2S}(z_p) \sim \frac{k^4}{M_5^3} \sigma_A^8 \sigma_S^2 \sigma^{-5}(z_p) \,. \tag{5.25}$$

Equating $\hat{\Gamma}_{A,2S}(z_p)$ with the actual rate (5.21) then gives

$$\frac{\sigma(z_p)}{\sigma_A} \sim \left[\frac{k^3}{M_5^3} \frac{\sigma_S^2}{\sigma_A^2} \right]^{1/5} \tag{5.26}$$

$$\ll 1 \,. \tag{5.27}$$

Put in words, we find that the penetration length z_p is longer than the A throat length z_A. Hence the imaginary part of the wavenumber in the SM throat, Im $\{\lambda^S\} \sim z_p^{-1}$, is much smaller than the real part Re $\{\lambda^S\} \sim \tilde{z}_A^{-1}$, which is what we wanted to show.

6 Level repulsion and crossing during SM throat relaxation

Recall that according to the conjecture of [11], the SM throat will be shortened during inflation by the effects of interactions of the A and the SM throat length modulus. After inflation ends, the SM throat should relax to its "full" length. While the quantitative details of the relaxation, such as its rate, are unknown, one can imagine modelling it via a time-dependent SM throat length z_S in the doubled RS model that we employ to represent the full string theory setup.

A changing SM throat length leads to an additional possible mechanism of energy transfer. As the length of the SM throat increases, it will periodically go through an interval where the lengths of the A and SM throats

are tuned in the sense that there is a (near) degeneracy between pairs of one level from each throat. As is usual in quantum mechanics, the energy levels of coupled systems avoid crossing each other, which in this case means that a level that started out as an A throat KK mode will, after passing through the tuning point, become an SM throat KK mode and vice versa. This mechanism could, if the SM throat relaxation is slow enough, "suck" the energy out of the A throat and into the SM throat, where the KK modes would quickly decay into lower-lying states that cannot switch back to the A throat. We start by presenting a simple version of this mechanism that neglects the presence of complex parts in the frequency and wavenumbers induced by mode decay; then we investigate whether properly accounting for the said complex parts changes the picture qualitatively.

We will assume that the SM throat relaxation is adiabatic, at least as far as the A throat KK modes (and SM throat modes of comparable masses) are concerned. The usual condition for adiabaticity, $\dot{\omega}/\omega^2 \ll 1$ implies, via $\tilde{z}_S\omega \approx$ const, a condition $\dot{z} \ll \sigma_A/\sigma_S$. We will simply assume this condition is satisfied. Let us now look at how the KK modes evolve with a changing z_S while $z_A =$ const. To get oriented, we first take the sink-less case of real $\lambda^A = \lambda^S = m$. The spectrum-generating matching condition (2.16) can be re-written in a more symmetric form as

$$\frac{Y_1 + Q_m^A J_1}{Y_2 + Q_m^A J_2} + \frac{Y_1 + Q_m^S J_1}{Y_2 + Q_m^S J_2} = 0\,, \tag{6.1}$$

where the Bessel functions are all evaluated at m/k and the coefficients Q are given by

$$Q_m^{A,S} = -\frac{Y_1(m\tilde{z}_{A,S})}{J_1(m\tilde{z}_{A,S})}\,. \tag{6.2}$$

Let us start with z_S such that the two throats are detuned (that is, only one of the coefficients Q is large). Recall that an A throat KK mode has a large Q_m^A and a small (~ 1) Q_m^S. As $\tilde{z}_S$ increases, the mode's mass remains approximately constant until Q_m^S starts becoming large as well. At this point the mass m starts moving such that $m\tilde{z}_S$ will remain approximately constant, Q_m^A will become small (~ 1) and Q_m^S will become large – what started as an A throat KK mode has become an SM throat mode. The switch-over will repeat itself in reverse when z_S decreases further and the throats become tuned again. Of course, if we had started by tracking an SM throat mode, it would switch over into the A throat at the first point of tuning, and then back to the SM throat at the second one. This is an example of a standard quantum-mechanical level repulsion: at each point where the two throats have tuned lengths, the levels of one A throat mode and one SM throat mode avoid crossing by switching their "home throat". In principle, this switching can facilitate energy transfer between the throats; if it is slow enough to allow the modes to fully relax, a KK mode particle originally located in the A throat will relocate to the SM throat where it can decay to lower KK modes very efficiently. If the A throat mode is the low-lying one, it is quite likely that the products of its decay will have masses below the lowest lying A throat KK mode and hence will not be subject to switching anymore.

This simple picture has an obvious loophole: when one takes into account the presence of the sink(s), the mode wavenumbers $\lambda^{A,S}$ acquire (different) imaginary parts and it becomes possible for the levels to avoid each other in the complex plane even though the real parts cross. It is easy to see that this will happen when the imaginary part of one of the wavenumbers is large: in that case the corresponding coefficient Q_m cannot become large (as we show below), meaning that the mode can never switch to that side. On the other hand, one would expect that if the sink(s), and hence the imaginary parts of the wavenumbers, are very small, the system should behave similarly to the one without sinks at all (in other words, the equations governing the eigenvalues are analytic and we do not expect any discontinuities for $S \to 0$). Hence there should be a maximum sink that still allows the mode switching to take place; above that sink the real parts of the wavenumbers can cross and modes remain in their respective throats. Let us find the condition for the switching to take place, and see whether our model satisfies it.

The spectrum is determined by (5.8). It is clear that as long as both the (real) mass m and the sink S are much smaller than the curvature scale k, the only way to satisfy (5.8) is to have at least one of the coefficients

Q_m large. Suppose we start with detuned throats and pick an A throat mode, *i.e.,* Q_m^A is large: to leading order,

$$Q_m^A \approx -\frac{\lambda^S Y_1^S Y_2^A + \lambda^A Y_1^A Y_2^S}{\lambda^A J_1^A Y_2^S} \sim \frac{k^2}{\lambda^2}\,, \tag{6.3}$$

where we have introduced a shortened notation for the Bessel functions by denoting $Y_1^S \equiv Y_1(\lambda^S/k)$ etc, and in the last expression we have neglected the difference between the wavenumbers. As we have noted before, (5.6) implies that λ^A must be (nearly) real.

For the mode to switch throats, Q_m^S must become of the same order at the tuning point (and then remain large afterwards). The expression (5.7) reduces, in the asymptotic regime, to

$$Q_m^S \approx -\cot(\lambda^S \tilde{z}_S + \text{const})\,, \tag{6.4}$$

where the const $= -\pi/4$ can be neglected for the purposes of our argument. Let us denote $\lambda^S \tilde{z}_S = a_S + i b_S$ with a_S, b_S real. We then have

$$Q_m^S \approx -\frac{\sin a_S \cos a_S - i \sinh b_S \cosh b_S}{\sin^2 a_S + \sinh^2 b_S}\,. \tag{6.5}$$

It is clear that if b_S is of order 1 or larger, Q_m^S will always be of order 1. Hence b_S will have to be small; we can then approximate $\sinh b_S \approx b_S$, $\cosh b_S \approx 1$. For small b_S the expression (6.5) will be largest when $\sin a_S \approx \beta_S$, and the maximum value attained will be $\sim 1/b_S$ (both the real and imaginary parts will attain values of this order). Comparing with the required order of magnitude (6.3) we find that switching can only occur when $b_S \lesssim |\lambda^2|/k^2$. This means that the imaginary part of the wavenumber itself must be tiny:

$$\begin{aligned} \text{Im}\,\{\lambda^S\} &= \frac{b_S}{\tilde{z}_S} \sim \frac{|\lambda_S^2|}{k^2 z_S} \\ &\lesssim k\sigma_A^2 \sigma_S \sim \frac{\sigma_A^2}{\tilde{z}_S}\,, \end{aligned} \tag{6.6}$$

where we have used that the typical value of the wavenumber is $\sim k\sigma_A$. This condition is not satisfied by our model: while (6.6) implies that the penetration length $z_p \sim (\text{Im}\,\{\lambda^S\})^{-1}$ must be much longer than the SM throat length z_S, at the end of Section 5.1 we have argued that the penetration length will be much shorter than the throat length (and the "self-consistent" penetration length obtained from (5.26) does indeed come out shorter than the SM throat length). Hence we conclude that the mode switching cannot occur.

7 Enhancing KK mode tunnelling between throats

In previous sections we have found that, generically, energy transfer between the throats will proceed at the rate given by the plane wave tunnelling rate of [14]. In this section we look for ways of enhancing the tunnelling rate by modifying the effective potential barrier in the UV region of the RS model. In standard RS the tunnelling probability of a mode of mass m (with $mL \ll 1$) is suppressed as [14]

$$P_{RS} \sim (mL)^4\,. \tag{7.1}$$

Throughout this section we will, for convenience, use curvature radii L instead of curvature scales k; they are straightforwardly related by

$$L \equiv \frac{1}{k}\,. \tag{7.2}$$

Since we are interested in plane wave tunnelling rates, we will work with the plane wave boundary conditions that are commonly used in tunnelling calculations, *i.e.,* the SM side wave function will be an asymptotically

purely outgoing wave $\sqrt{m\widetilde{z}}H_2^+(m\widetilde{z})$. On the A side we will have a mix of incoming and outgoing waves (with a nonzero net incoming flux), $\sqrt{m\widetilde{z}}H_2^-(m\widetilde{z})$ and $\sqrt{m\widetilde{z}}H_2^+(m\widetilde{z})$ respectively, where

$$H_\nu^\pm(x) = J_\nu(x) \pm iY_\nu(x) \tag{7.3}$$

are the usual Hankel functions. Unlike the Z_2 boundary conditions employed in previous sections, the tunnelling ones do not explicitly depend on the location of the end-branes. We will not take into account the effects of decay here; the decay effects can be obtained by a straightforward adaptation of the results of previous sections.

Our aim of lowering the potential barrier will be achieved by replacing the (single) UV brane with tension (2.5) by a certain number, N, of branes with smaller tension

$$T' = T/N\,. \tag{7.4}$$

Such "generalized Randall–Sundrum" setups were considered, *e.g.,* in [18, 19]. If N is small, say 2, tunnelling can be speeded up by resonant effects akin to the resonant tunnelling phenomenon known from ordinary quantum mechanics (resonant tunnelling was also discussed by [12, 13]); we give an explicit example of such a setup in Section 7.3. On the other hand, a large number of appropriately placed branes will lower the effective potential barrier and hence enhance tunnelling, as we show in Section 7.5. All cases will have in common the fact that the curvatures on the two sides of any particular membrane differ; therefore we will start with a general discussion of the matching conditions for such situations.

7.1 Many-brane Randall–Sundrum

Let us assume that our system consists of N AdS regions bounded by $N+1$ branes located at $z = z_i, i = 0, .., N$. The brane at z_0 will be taken to be the annihilating brane that are responsible for inflation, while the one at z_{N+1} will be the SM brane. In each region between the branes the metric is the standard AdS metric (2.2), but the warp factor will have different coefficients in each region, namely

$$\sigma_i(z) = \frac{L_i}{z + \widetilde{L}_i}\,. \tag{7.5}$$

The variables L_i are (up to sign) the curvature radii of each region. The sign of L_i will be positive (negative) if the warp factor decreases (increases) with increasing z. The shifts $\widetilde{L}_i$ are chosen such that the warp factor is continuous at every membrane. The actual values of $\widetilde{L}_i$ depend on a choice of the origin of the z coordinate and the normalization of the warp factor.

The curvature jump conditions at each of the branes require that the reduced tension $\widetilde{T}_i \equiv T_i/M_5^3$ of brane i and the curvature parameters L_i and L_{i+1} on both sides of the membrane satisfy (cf. (2.5))

$$\widetilde{T}_i = 12\left(\frac{1}{L_{i+1}} - \frac{1}{L_i}\right)\,. \tag{7.6}$$

This condition is valid both at the interior branes as well as at the inflating and SM branes, the only difference being that at the latter two we also impose Z_2 boundary conditions on the background.

The mode equation in each region has the same form as in the single UV brane case, namely (2.8), but with the potential $V(z)$ now given by

$$V(z) = \frac{15}{8}\frac{1}{\left(z + \widetilde{L}_i\right)^2}\,, \qquad z_{i-1} < z < z_i\,. \tag{7.7}$$

Each brane will contribute a term of the form

$$V_i^{(b)} = \widetilde{T}_i\sigma(z_i)\delta(z - z_i) \tag{7.8}$$

into the effective potential as well.

Away from the branes in each region the KK wave functions $\psi_m(z)$ are given by a general combination of the Bessel functions $J_2(m\widetilde{z}_i(z))$ and $Y_2(m\widetilde{z}_i(z))$, where

$$\widetilde{z}_i(z) \equiv |z + \widetilde{L}_i| \,. \tag{7.9}$$

At each membrane the wave function ψ_m must be continuous,

$$\psi_m(z \to z_i^-) = \psi_m(z \to z_i^+) \,, \tag{7.10}$$

and its derivative must obey the jump condition

$$-\frac{1}{2\psi_m(z_i)} \left[\partial_z \psi_m(z_i^+) - \partial_z \psi_m(z_i^-)\right] = \frac{\widetilde{T}_i}{16}\sigma(z_i) \,. \tag{7.11}$$

The zero mode wave function is a direct generalization of (3.4): in i-th region it is

$$\psi_0(z) = N_i \frac{1}{(\widetilde{z}_i(z))^{3/2}} \,, \tag{7.12}$$

where the normalization constants N_i are chosen such that the wave function is continuous across every membrane.[11] In fact, since the warp factor σ has the same functional form and coefficients that do make it continuous, we can also write

$$\psi_0(z) = N_0 \sigma^{3/2}(z) \,, \tag{7.13}$$

where the normalization constant N_0 is now the same for all regions.

7.2 Throats with different curvature radii

An interesting generalization of the models of [9, 14] is to allow the curvature radii of the two throats to differ. The radii can in principle arbitrary as long as the tension of the brane that separates them obeys the jump condition (7.6). Let us first look at the plane wave tunnelling rate through a one-brane potential barrier that separates two regions with curvature radii L^A and L^S, respectively. Normalizing the warp factor to 1 at the UV brane ($z = 0$) leads to $\widetilde{L}^A = L^A$, $\widetilde{L}^S = L^S$ (see (7.5)). The KK mode wavefunctions on the A and SM sides are, respectively,

$$\psi^A(z) = \sqrt{m\tilde{z}_A}\left[AH_2^-(m\tilde{z}_A) + BH_2^+(m\tilde{z}_A)\right] \,, \tag{7.14}$$

$$\psi^S(z) = \sqrt{m\tilde{z}_S} C H_2^+(m\tilde{z}_S) \,, \tag{7.15}$$

where

$$\tilde{z}_{A,S} = |z + L^{A,S}| \,. \tag{7.16}$$

As usual, on the A side we have a superposition of an incoming and a reflected wave, whereas on the SM side only the transmitted component is present. Continuity and first derivative jump at the brane, (7.10) and (7.6), lead to

$$\frac{C}{A} = \sqrt{\frac{L^A}{L^S}} \frac{H_2^-(mL^A)H_1^+(mL^A) - H_1^-(mL^A)H_2^+(mL^A)}{H_2^+(mL^S)H_1^+(mL^A) + H_2^+(mL^A)H_1^+(mL^S)} \,. \tag{7.17}$$

Let us first assume that the curvature radii are such that $mL^A \ll 1, mL^S \ll 1$. Then, using the small-argument expansions of Bessel functions (A.1), we find

$$\left|\frac{C}{A}\right| \sim m^2 (L^A)^{3/2} (L^S)^{1/2} \,. \tag{7.18}$$

[11] The proper jump in the first derivative then follows automatically.

Hence, making L^S moderately larger than L^A can increase the plane wave tunnelling rate somewhat, but not by a lot.

Next, let us assume that the SM curvature radius is large, such that $mL^S \gtrsim 1$. The Hankel functions can then be characterized as $H_\nu^\pm(mL^S) \sim e^{\pm imL^S}/\sqrt{mL^S}$, and we find

$$\left|\frac{C}{A}\right| \sim (mL^A)^{3/2}\,. \tag{7.19}$$

In particular, this formula also applies when $L^S \to \infty$, that is when the SM side of the UV membrane is flat, and so characterizes the tunnelling of KK modes out of a single AdS_5 throat. Compared to the equal radii case $L^A = L^S$, the tunnelling rate $P = |C/A|^2$ is clearly enhanced by a factor of $1/(mL^A)$.

Having significantly different radii in the two throats has other interesting consequences: for example, it can relax the constraint (3.29) on the relative sizes of the warp factors at the A and SM branes – the derivation of the constraint from (3.28) (which remains valid even in the case of different curvature radii) assumed equal curvature radii on both sides. Conversely, if the curvature radius L^S of the SM throat were much larger than L^A, the SM warp factor $\sigma_S \equiv L^S/(L^S + z_S)$ could be much larger than the bound (3.29) while allowing KK modes to tunnel from the A throat to the SM one. Phenomenologically, however, such a setup may not be desirable because of the presence of a large hierarchy between the curvature scales in two throats; it may also be difficult to realize such a setup as a string theory compactification.

7.3 Resonant tunnelling through a gravity box

One possibility to speed up the energy transfer between throats is to use an analog of the resonant tunnelling effect from standard quantum mechanics: split the single potential barrier (the UV region) in the RS geometry into two, with a flat region (a well with zero potential in the effective Schrödinger equation) inbetween [15]. If the frequency of the tunnelling wave is tuned to the size of the of the well in the middle, the tunnelling rate can approach one. As argued in [12, 13] who analyzed a similar setup, in a realistic string theory compactification one would expect that the two throats are joined by a bulk region that is modelled by the flat interval.

Hence we consider a setup of the type described in [15], but with the tunnelling boundary conditions. The geometry consists of two AdS throats, whose curvatures we will take to be the same for simplicity, separated by a flat region. The curvature radius of the throats will be denoted by L, while the length of the box in the middle will be $2l$, with the branes sitting at $z = \pm l$. The effective potential is plotted in Fig 1 (a). The warp factor is constant in the central region and will be normalized to 1 there (so the coordinate and proper length of the middle box coincide). On the A side (region 1) the wave function of a KK mode with mass m is

$$\psi_m^{(1)}(z) = \sqrt{m\widetilde{z}_1(z)}\left[AH_2^+(m\widetilde{z}_1(z)) + BH_2^-(m\widetilde{z}_1(z))\right], \tag{7.20}$$

while in the middle box (region 2) the wave function is

$$\psi_m^{(2)}(z) = C\cos(mz) + D\sin(mz)\,, \tag{7.21}$$

and on the SM side (region 3) we have

$$\psi_m^{(3)}(z) = \sqrt{m\widetilde{z}_3(z)}EH_2^+(m\widetilde{z}_3(z))\,. \tag{7.22}$$

In the notation of Section 7.1 the parameters L_i are

$$L_3 = -L_1 = L, \quad L2 = \widetilde{L}_2 \to \infty\,, \tag{7.23}$$

while the shifts are (from requiring $\sigma(z = \pm l) = 1$)

$$\widetilde{L}_1 = -\widetilde{L}_3 = -L + l\,. \tag{7.24}$$

It is straightforward, if somewhat tedious, to solve the matching conditions (7.10) and (7.11). To shorten the result, let us denote

$$t \equiv \tan ml \,, \tag{7.25}$$

and omit the arguments of all Hankel functions, since they are all evaluated at mL. The tunnelling amplitude E/B is then

$$\frac{E}{B} = \frac{1}{2} \frac{\left(t + \frac{1}{t}\right)\left(H_2^- H_1^+ - H_1^- H_2^+\right)}{{H_2^+}^2 - {H_1^+}^2 + \left(\frac{1}{t} - t\right) H_2^+ H_1^+} \,. \tag{7.26}$$

As a check, when $t \to 0$, so $1/t$ dominates over everything else, the above tunnelling amplitude reduces to the bulk-less expression given in [14].

The tunnelling resonance occurs when the denominator becomes small, *i.e.,* when

$$\frac{1}{t} - t \approx \frac{{H_2^+}^2 - {H_1^+}^2}{H_2^+ H_1^+} \,. \tag{7.27}$$

If we concentrate on KK modes whose mass m is small compared to the inverse curvature radius, $mL \ll 1$, we can use the asymptotic forms (A.1) of the Bessel functions, and we find that the denominator becomes small when

$$\frac{1}{t} - t \sim mL \ll 1 \,, \tag{7.28}$$

that is when $t \approx 1$. This is not surprising – it means that to get an amplification of the tunnelling rate, the size of the central box must be roughly the same as the wavelength of the tunnelling particle. As a numerical illustration, we plot the potential and the tunnelling rate of this setup in Fig. 1. The parameters used in the plot are $l = 5$, $L = 1$.

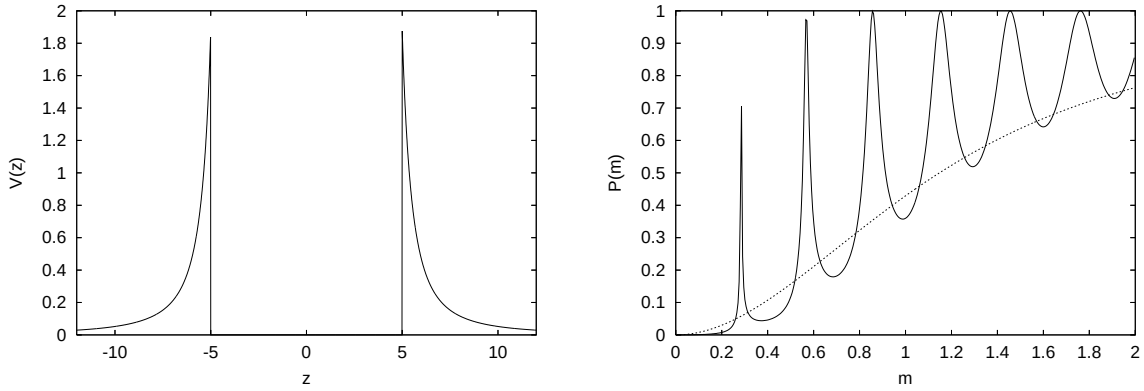

(a) (b)

Figure 1: Two branes with a flat region between them. Graph (a) plots the potential $V(z)$, while (b) shows the tunnelling rate P as a function of the KK mode mass m (solid line) together with the reference tunnelling rate of the standard double RS geometry (dotted line). The brane separation is $2l = 10$. Tunnelling is greatly enhanced for masses that fall within the resonant tunnelling peaks. Note also the suppression of the tunnelling rate for very light modes.

This is bad news for phenomenology. According to the discussion around Eq. (2.21) we would expect the masses of the produced KK modes to be smaller than the annihilation scale M_A, which in turn is expected to be a few orders of magnitude lower than the inverse curvature radius L of the throats. Hence, the flat region

would have to be unnaturally long as compared to the characteristic length of the throats, and presumably as compared to the radius of the internal manifold in a string theory compactification; in other words, the hierarchy problem that the warping was supposed solve would reappear in a different guise.

Lastly, one can consider the regime of t small but not too small; more precisely,

$$1 \gg t \gg \frac{Y_1(mL)}{Y_2(mL)} \sim mL\,. \tag{7.29}$$

In this regime the tunnelling amplitude behaves roughly as

$$\frac{E}{B} \sim \frac{mL}{t}(mL)^2\,, \tag{7.30}$$

meaning that the tunnelling rate with bulk present is suppressed by an additional factor of $(mL/t)^2$ compared to the bulk-less tunnelling rate. The extra suppression is also evident in the plot 1(b).

7.4 Comments on the WKB approximation

Incidentally, our results (7.19) and (7.30) provide a cautionary note on the WKB methods used, *e.g.*, by [12, 13]. In the WKB approximation, when the tunnelling amplitudes are small, the tunnelling amplitude Θ_{tt} between two throats is roughly given by the square of the rate Θ_{tb} at which particles can tunnel from one throat into (flat) bulk,

$$\Theta_{tt} \approx \Theta_{tb}^2\,. \tag{7.31}$$

It is clear that such formulae must be used with caution: for example, the tunnelling amplitude between two RS throats, calculated in [14], is $\Theta_{tt} \sim (mL)^2$, while the throat-to-bulk tunnelling amplitude (7.19) is $\Theta_{tb} \sim (mL)^{3/2}$. Further, when the two throats are separated by a flat bulk region, the tunnelling amplitude (7.29) does formally exhibit the $(mL)^3$ behaviour that one would expect from Θ_{tb}, but it also depends on the length of the bulk region represented by the parameter t (and the dependence is very different from the WKB approximation as used in [12, 13]).

7.5 Lowering the potential barrier by multiple branes

Another way of speeding up the tunnelling process is to lower the potential barrier in the UV region by replacing the single UV brane by a large number of branes of lower tension that are also spatially separated along the z direction. The basic idea is to utilize the fact that the (squared) warp factor $\sigma_i^2(z)$ and the potential $V(z)$, given respectively in (7.5) and (7.7), differ by a factor of the (squared) curvature radius L^2. By arranging the branes such that the the warp factor becomes of order 1 only when the curvature radius is also large, we can achieve a significant lowering of the effective potential barrier between the throats.

We have not attempted an exhaustive search for the configuration most favourable for tunnelling. It is clear nevertheless that the the modification must happen in the region where the warp factor (and the Randall–Sundrum potential) are large, namely around $z = 0$. In this section we present a toy example of such a modification.

Suppose we arrange $N = 2n$ branes with tension $\widetilde{T}_1 = \widetilde{T}/N$ such that the middle region is (approximately) flat. Then the curvature radius of a region i satisfies

$$\frac{1}{L_i} = 12\widetilde{T}_1(i-n)\,. \tag{7.32}$$

As discussed above, $1/L_i^2$ is precisely the factor (up to 15/8) by which the potential and the warp factor differ:

$$\begin{aligned} V_i(z) &= \frac{15}{8}\frac{\sigma_i^2(z)}{L_i^2} \\ &= \frac{15}{8}\left(12\widetilde{T}\sigma_i(z)\right)^2\frac{(i-n)^2}{N^2}\,. \end{aligned} \tag{7.33}$$

The last expression makes the suppression of the potential more apparent: the warp factor is largest in the middle (flat) region, but the potential there is suppressed by the $(i-n)^2/N^2$ factor. Because the shifts $\widetilde{L}_i$ entering the warp factor are determined recursively, it is not possible to derive a simple formula for the maximum of the potential (7.33), so we give a few simple examples for illustration.

In our example, we fix the warp factor value at the maximum to be 1. This choice ensures that the warping at the "top" of the throats is the same for all setups — while arbitrary, this has the physical consequence of measuring masses at the top of the throats in the same units. Further, since we consider a many-brane scenario to be a near-the-top modification of the "standard" model of [9, 14], we fix the curvature and warp factors at the bottom of the throats to be the same in all cases.

In Fig. 2 we show potential as a function of the coordinate z and the tunnelling rate as a function of the mass m of the tunnelling KK mode for the benchmark doubled RS (*i.e.,* constant-curvature, single central brane) setup of [9, 14]. As expected, the tunnelling rate becomes substantial when the KK mode mass m^2 becomes the same as the potential at the top of the barrier.

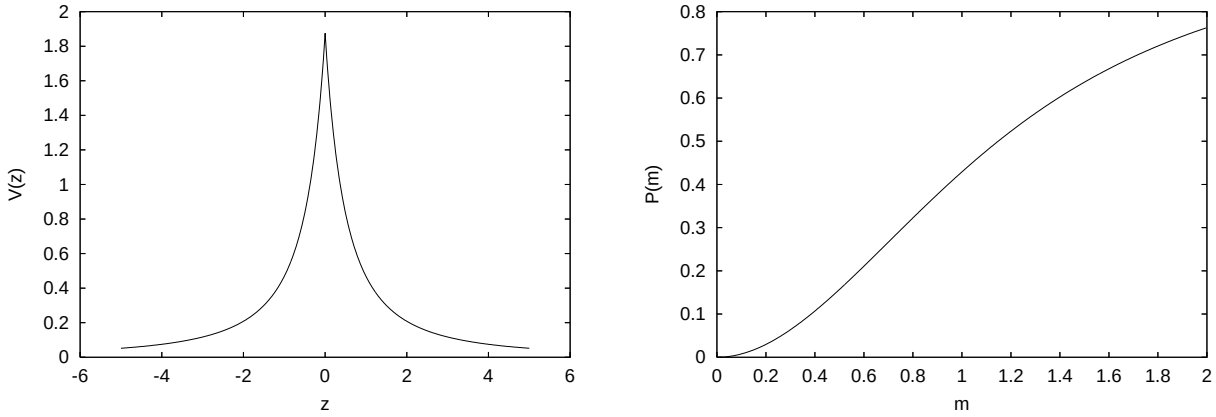

(a) (b)

Figure 2: The single central brane setup with constant curvature. Graph (a) plots the potential $V(z)$, while (b) shows the tunnelling rate as a function of the KK mode mass m.

Now let us look at a setup where the central brane is replaced by 100 equidistant branes (50 on each side of $z=0$) with tension equal 1/100 of the tension of the single brane. The potential and the tunnelling rate are shown in Fig. 3. In Fig. 4 we zoom in on the central region to show the potential in more detail. The potential barrier is significantly lower and the tunnelling rate for low-lying KK modes is correspondingly enhanced.

Are the implications of this toy model applicable to an honest string theory compactification? Recent work [12, 13] studying string theory throats seem to answer this question in the negative. We would like to take a more cautious position: it seems clear that the tunnelling rates depend to a large degree on the details of the gluing of the throat to the bulk; these details that are not yet under sufficient control. In fact, the effective potentials for the KK modes in [12, 13] and our potential plotted in Fig. 3 are qualitatively similar, but their quantitative details are apparently sufficiently different to cause a major difference in tunnelling rates.

8 Conclusions

We have presented an exhaustive discussion of the properties of the KK modes that are responsible for the energy transfer from the A throat to the SM throat. We have found that tunnelling in the conventional sense will proceed only if the SM throat is substantially longer than the A throat, namely only for $z_S \gtrsim z_A(k\tilde{z}_A)^4$.

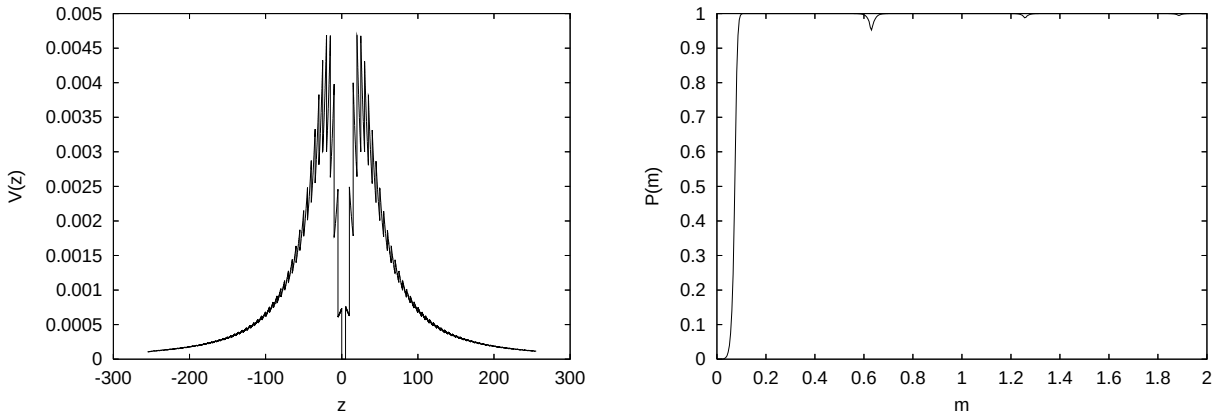

(a) (b)

Figure 3: The multiple brane setup. Graph (a) plots the potential $V(z)$, while (b) shows the tunnelling rate as a function of the KK mode mass m.

Even when the A throat KK modes do not tunnel in the conventional sense, their wavefunction has a tail in the SM throat that is big enough to induce a large decay rate into 2 SM throat KK modes. Naively this rate should increase with the length of the SM throat and, for a long SM throat, will be large enough to make most of the annihilation KK mode energy go into SM throat KK modes. However, a more careful analysis taking into account the effects of wavefunction decay shows that the decay rate into two SM throat KK modes cannot get larger than a certain maximum. The effect can be understood intuitively from the fact that a large decay rate would shorten the penetration length of the A throat KK mode into the SM throat, which in turns leads to a suppression of the overlap of its wavefunction with the SM throat KK modes, and that in turn suppresses the decay rate. We have shown that the physically realized decay rate is effectively given by the plane wave tunnelling rate. Nevertheless, the naive decay rate is *not* completely meaningless: we show that it is turn small enough that it does not induce a further slowing down of the tunnelling/decay rates via the complex frequency effect discussed in [10].

An additional mechanism of energy transfer we have investigated is based on level repulsion and can be pictured as throat switching by KK modes when the spectrum of the SM throat is gradually lowered by the relaxation of the SM throat. We found that the presence of complex parts in the mode frequencies destroys the level repulsion effect, because levels can now avoid each other in the complex plane; hence, the energy transfer by switching cannot occur.

We have then proposed a simple modification of the UV region of the geometry that, at least in the phenomenological 5-dimensional model, leads to a drastic enhancement of tunnelling rates between the two throats. The modification consists of replacing a single UV brane with an array if branes with lower tension such that the curvatures deep in the throats remain the same. This has the effect of lowering the potential in the effective Schrödinger equation that the KK modes have to tunnel through, leading to an enhancement of their tunnelling rates. It is not clear, especially in the light of the recent studies of stringy throats [12, 13], whether a similar mechanism could be realized in an honest string compactification; we argued that a better knowledge of the geometry where the throats are glued to the bulk is necessary to answer this question definitely.

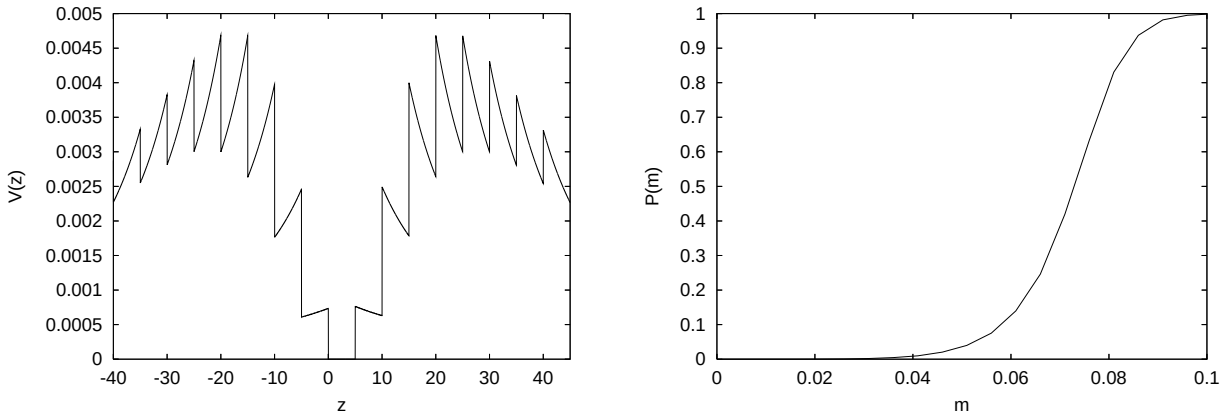

(a) (b)

Figure 4: Detail of (a) the potential $V(z)$ and (b) the tunnelling rate $P(m)$ shown in Fig. 3.

Acknowledgements

It is a pleasure to thank Rob Myers for many key discussions and suggestions, and Xingang Chen, Jean Francois Dufaux, Hassan Firouzjahi, Lev Kofman, Dmitry Podolsky, Gary Shiu, Henry Tye and Bret Underwood for interesting discussions. The author is supported by an NSERC Discovery grant. Research at the Perimeter Institute is supported in part by funds from NSERC of Canada and MEDT of Ontario.

A Modes of a two-throat system

In this appendix we study in detail the modes of the two-throat system described in Section 3.1.

A.1 Small mass modes: $mz_A \ll 1$

Taking the mass to be small allows us to use standard formulae for Bessel functions of small arguments, namely

$$\begin{aligned} Y_1(x) &\approx -\frac{2}{\pi}\frac{1}{x} & Y_2(x) &\approx -\frac{4}{\pi}\frac{1}{x^2} \\ J_1(x) &\approx \frac{1}{2}x & J_2(x) &\approx \frac{1}{8}x^2\,. \end{aligned} \tag{A.1}$$

We then have

$$Q_m^A \approx \frac{4}{\pi}\frac{1}{(m\widetilde{z}_A)^2} \tag{A.2}$$

$$Q_m^S \approx -\frac{8}{\pi}\frac{k^2}{m^2} \tag{A.3}$$

$$N_m^S \approx \frac{\pi}{8}\left(\frac{m}{k}\right)^2 \tag{A.4}$$

$$N_m^A \approx N_m^S \tag{A.5}$$

$$\psi_m^A(z_A) \approx \frac{1}{2}\sqrt{\frac{m}{k}}\frac{1}{(k\widetilde{z}_A)^{3/2}} \tag{A.6}$$

and find

$$R_\psi \equiv \frac{\psi_m^A(z_A)}{\psi_0(z_A)} \approx \frac{1}{2}\frac{\sqrt{m}}{k}\,. \tag{A.7}$$

One should not be surprised that this ratio is not dimensionless; after all, we are comparing wavefunctions that have different (namely continuum vs. discrete) normalizations. Physically one cannot talk about a single mass value (or mode) out of a continuum; one must always integrate over a certain range of masses to get a meaningful result. One can, *e.g.,* integrate the probability density of finding a KK mode of mass $m' < m$ at the A brane and compare it to the probability density of finding the zero mode there, *i.e.,* calculate

$$p(m) = \frac{\int_0^m dm' \left(\psi_{m'}^A(z_A)\right)^2}{\psi_0^2(z_A)}\,. \tag{A.8}$$

Using (A.7) we find

$$p(m) \approx \frac{1}{4}\frac{m^2}{k^2}\,. \tag{A.9}$$

As derived, this expression is only valid for $m \ll 1/z_A$. We would like to extend this calculation to modes whose mass is of order $1/z_A$, because we expect that the effective brane scale M_A will be roughly of that magnitude.

A.2 Medium mass modes: $mz_A \sim 1$

There is no good approximation formula for the Bessel functions when their arguments are of order 1; the best one can do is to say that generically, all of the relevant Bessel functions are also of order 1. Thus one cannot say much more about Q_m^A than that it will also generically be of order 1. That is enough, however, to fix Q_m^S by the jump condition at the Planck brane (recall that we still assume $mk \ll 1$, so all Bessel functions evaluated at the Planck brane can be replaced by their small-argument approximations). We find that Q_m^S, and therefore also the normalization constants N_m^S and N_m^A are given by the same expressions as in the small mass case, namely (A.3)—(A.5). The wavefunction of the massive mode at the A brane is then[12]

$$\psi_m^A(z_A) \sim \frac{m^{5/2}\widetilde{z}_A^{1/2}}{k^2} \tag{A.10}$$

Interestingly enough, the ratio $\psi_m^A(z_A)/\psi_0(z_A)$ is then (using $m\widetilde{z}_A \sim 1$) roughly the same as in the small mass case, namely

$$R_\psi = \frac{\psi_m^A(z_A)}{\psi_0(z_A)} \sim \frac{\sqrt{m}}{k}\,. \tag{A.11}$$

We show below that this result holds only for truly "generic" values of m; we will see below that at special points, the ratio R_ψ can grow to be much larger than the above value.

The result (A.11) implies that one can integrate up to $m \sim z_A$ in (A.8) with result

$$p(m) \sim \left(\frac{m}{k}\right)^2\,, \tag{A.12}$$

that is the non-zero mode amplitude at the A brane is suppressed by roughly the square of the ratio of the inflation and string scales (modulo the radius of the 5th dimension).

Since in this case we do not have factors of order one under control, it is useful to plot the $\psi_m^A(z_A)/\psi_0(z_A)$ numerically. The plot can be found in Fig. 5(a).

To see that the validity of our approximations is restricted to "generic points", let us look at plots of the ratio R_ψ for values of m that are several times $1/z_A$. The plot in Fig. 5(b) shows that for certain masses,

[12] We use the $\sim$ sign to denote our ignorance of factors of order 1 (we reserve $\approx$ for approximations that hold up to small corrections).

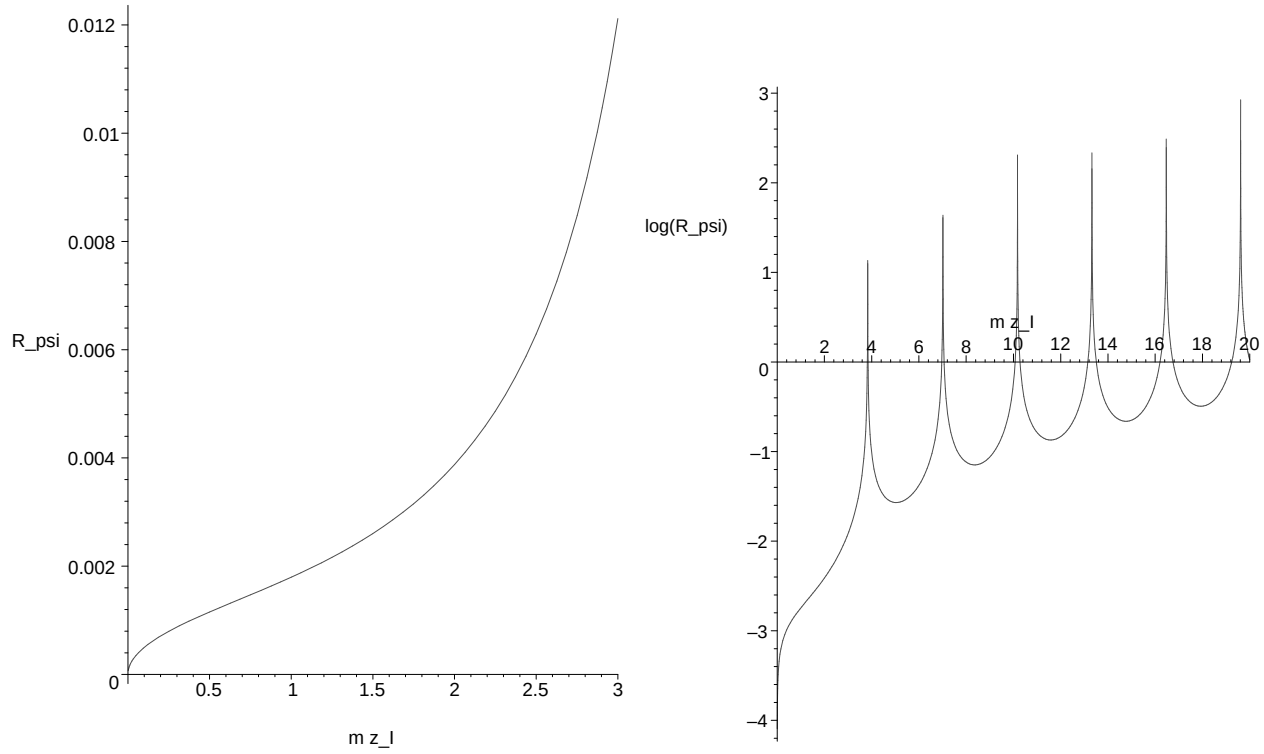

Figure 5: Plot (a) shows the ratio $R_\psi = \psi^A_m(z_A)/\psi_0(z_A)$, as a function of m (in units of $1/z_A$). For small m the ratio behaves as $\sim \sqrt{m}/k$. In this plot $k = 1, z_A = 10^5$. In (b) we plot the logarithm of the ratio $R_\psi = \psi^A_m(z_A)/\psi_0(z_A)$, as a function of m (in units of $1/z_A$), for a larger range of m. This plot is logarithmic, so the KK mode wavefunctions are suppressed with respect to the zero mode whenever the curve is below the horizontal axis. Note the presence of spikes that actually turn out to dominate the integrated ratio $p(m)$.

the wave function of the corresponding modes on the A brane is parametrically amplified. One might suspect that these spikes in R_ψ appear when either Q^A_m diverges (at the zeros of $J_1(m\widetilde{z}_A)$), or the denominator in the expression (2.18) for N^A_m becomes zero, and R_ψ would diverge. In fact, it turns out that neither of these special points can cause the spike; rather, the spikes appear at values for which Q^S_m approaches zero, and R_ψ remains bounded (but large). For $m \ll k$ one can use the approximate values (A.1) of the Bessel functions to show that at the points where $Q^S_m = 0$, the KK mode wave functions attain values $\sim k^2/m^2$, and the ratio R_ψ grows to $R_\psi \sim (k/m)^{7/2}/\sqrt{k}$.

Physically, the interesting question is for what values of m does the integrated probability density ratio $p(m)$ of (A.8) reach values ~ 1. The presence of the spikes makes a numerical integration difficult, so we provide estimates that will turn out to be good enough. We start with generic values of m and consider the contribution of the spikes separately below.

For a values of the KK mode mass m away from the spikes, the approximate form (A.10) holds as long as $m < k$. Keeping z_A in the expressions explicitly, we arrive at

$$R_\psi \sim \frac{\sqrt{m}}{k}\,(mz_A)^2\,, \tag{A.13}$$

and

$$p(m) \sim \frac{m^2}{k^2} (m z_A)^4 \,. \tag{A.14}$$

This result is counterintuitive: it says that for the KK modes to dominate over the zero mode, their mass must be so large that they are already far into their asymptotic regime, $m \gg 1/z_A$. However, in the asymptotic regime we would expect the KK modes to dominate over the zero mode, because the KK modes approach plane waves with constant magnitude, whereas the zero mode falls off as a power of z. We seem to be missing some KK mode contributions; this discrepancy is a hint that the spikes contribute significantly, and actually dominate $p(m)$. Let us now show that.

As we have already mentioned, the spikes appear at masses $\bar{m}$ such that $Q^S_{\bar{m}} = 0$. We remind the reader that we still assume $\bar{m} \ll k$. From (2.16) we find that the corresponding $Q^A_{\bar{m}}$ must be

$$Q^A_{\bar{m}} \approx -2 \frac{Y_1(\bar{m}/k)}{J_1(\bar{m}/k)} \sim \frac{k^2}{\bar{m}^2} \gg 1 \,. \tag{A.15}$$

This equation together with (2.14) determines the values of $\bar{m}$ where the spikes occur; the first few spikes will be at $\bar{m} \sim 1/z_A \ll k$ in accord with our assumption. It is also worth noting that the spike occurs when $J_1(m\widetilde{z}_A)$ is small but not zero, $J_1(m\widetilde{z}_A) \sim 1/Q^A_{\bar{m}} \sim \frac{\bar{m}^2}{k^2}$. From (2.17) we find

$$N^S_{\bar{m}} = 1 \,, \tag{A.16}$$

and from (2.18), taking into account (A.15)

$$N^A_{\bar{m}} \approx N^S_{\bar{m}} \,. \tag{A.17}$$

To estimate the contribution to $p(m)$ from a spike, we will find its width δm at half maximum. The relevant quantity here is $R^2_\psi(m) = \psi^2_m(z_A)/\psi^2_0(z_A)$, so half maximum is the point where the KK mode wavefunction squared ψ^2_m drops to half its peak size. The drop can come from two sources (see (2.10)): either N^A_m or Q^A_m can halve. Let us for now assume that N^A_m varies faster, find the width δ_m and then show that the variation in Q^A_m due to δ_m is smaller.

Hence, we are looking for δ_m such that for $m = \bar{m} + \delta m$, $(N^A_m)^2 = (N^A_{\bar{m}})^2/2$. This implies $(N^S_m)^2 = (N^S_{\bar{m}})^2/2$ and hence

$$Q^S_m = 1 \,. \tag{A.18}$$

Keeping only the leading terms in (2.16) (recall again $m/k \ll 1$) we find that Q^A_m must change from the $-2Y_1(m/k)/J_1(m/k)$ of (A.15) to

$$Q^A_m \approx \frac{2Y_1(m/k) - J_1(m/k)}{J_1(m/k)} \approx Q^A_{\bar{m}} - 1 \tag{A.19}$$

that is $\delta Q^A_m \approx -1$. Recall that $Q^A_{\bar{m}}$ is large because $J_1(\bar{m}\widetilde{z}_A)$ is near its zero; thus δQ^A_m will come from the change in $J_1(m\widetilde{z}_A)$ caused by δm, while $Y_1(m\widetilde{z}_A)$ remains approximately constant. Denoting the change in $J_1(m\widetilde{z}_A)$ by δJ_1, we require

$$\frac{Y_1(\bar{m}\widetilde{z}_A)}{J_1(\bar{m}\widetilde{z}_A) + \delta J_1} \approx Q^A_m \stackrel{!}{=} Q^A_{\bar{m}} - 1 \approx \frac{Y_1(\bar{m}\widetilde{z}_A)}{J_1(\bar{m}\widetilde{z}_A)} - 1 \tag{A.20}$$

leading to

$$\delta J_1 \approx \frac{J^2_1(\bar{m}\widetilde{z}_A)}{Y_1(\bar{m}\widetilde{z}_A)} \,. \tag{A.21}$$

Taking into account $Y_1(\bar{m}\widetilde{z}_A) \sim 1$ we have $J_1(\bar{m}\widetilde{z}_A) \sim (Q^A_{\bar{m}})^{-1}$, leading to

$$\delta J_1 \sim \frac{\bar{m}^4}{k^4} \,. \tag{A.22}$$

The last step is to write $\delta J_1 \approx \delta m z_A J_1'(\bar{m}\widetilde{z}_A) \sim \delta m \widetilde{z}_A$ (the derivative of J_1 near zero is ~ 1) giving

$$\delta m \sim \frac{\bar{m}^4}{k^4}\frac{1}{\widetilde{z}_A}\,. \tag{A.23}$$

Thus each spike will contribute roughly

$$\begin{aligned}\delta p &\sim \delta m\, R_\psi^2(\bar{m}) \\ &\sim \frac{k^3}{m^3}\frac{1}{k\widetilde{z}_A}\end{aligned} \tag{A.24}$$

into the integrated wave function ratio $p(m)$. If we concentrate on the first few spikes where $m\widetilde{z}_A \sim 1$, we can also express δp as

$$\begin{aligned}\delta p &\sim \frac{k^2}{m^2} \\ &\sim (k\widetilde{z}_A)^2 \\ &\approx \sigma_A^{-2}\,.\end{aligned} \tag{A.25}$$

The last form is particularly interesting - this is precisely the enhancement factor used in the literature [8, 9, 10].

B (Non-)Tunnelling between two wells in quantum mechanics

In Section 3.3 we have stumbled on a surprising fact: particles will not tunnel from the shorter into the longer throat unless the longer throat is substantially longer; in the AdS throat case we found that ratio of the throat coordinate lengths, z_S/z_A, had to obey

$$\frac{z_S}{z_A} > \left(\frac{k}{m}\right)^4\,. \tag{B.1}$$

A natural question of interpretation arises: in general, given a potential barrier between two wells, how much longer must the target well be for particles to tunnel from the source well? The answer is quite important in the context of warped reheating where the potential in the UV region presumably differs from the simple doubled RS model; if such a modification changes the above inequality (or, equivalently, (3.28)), the conclusions of Section 3.3 would be changed as well.

To gain some insight into the problem, let us consider a simple 1-dimensional quantum mechanical problem of two wells separated by a δ-function potential barrier located at $z = 0$,

$$U(z) = U_0\delta(z)\,. \tag{B.2}$$

In analogy with the two throat model we call one of the wells, for $z < 0$, the "annihilation" well and make it of length z_A, the well on the positive side will be called the Standard Model (SM) well and will have length z_S. Note that z_A and z_S correspond to their respective namesakes in the two-throat model which are coordinate lengths, not the physical lengths $y \sim \ln z$. Hence we will be studying the Schrödinger equation

$$\left[-\frac{1}{2}\frac{d^2}{dz^2} + U_0\delta(z)\right]\psi(z) = \frac{1}{2}E^2\psi(z) \tag{B.3}$$

with the boundary conditions

$$\psi(z = -z_A) = \psi(z = z_S) = 0\,. \tag{B.4}$$

At $z = 0$ we require continuity,

$$\psi(z = 0^+) = \psi(z = 0^-)\,, \tag{B.5}$$

and the appropriate jump in the first derivative,

$$\frac{1}{2}\frac{\psi'(0^+)-\psi'(0^-)}{\psi(0)} = U_0\,. \tag{B.6}$$

Analogously to the AdS case, let us denote the wave function corresponding to energy E by ψ_E; for clarity, we will write $\psi_E(z) = \psi_E^A(z)$ for $z<0$ and $\psi_E(z) = \psi_E^S(z)$ for $z>0$. The Schrödinger equation (B.3) away from $z=0$ has the solution (taking into account the boundary conditions (B.4))

$$\begin{aligned}\psi_E^A(z) &= N_E^A \sin[E(z+z_A)]\\ \psi_E^S(z) &= N_E^S \sin[E(z-z_S)]\,.\end{aligned} \tag{B.7}$$

The matching conditions at $z=0$ then imply

$$N_E^A \sin Ez_A = -N_E^S \sin Ez_S\,, \tag{B.8}$$

$$\cot Ez_A + \cot Ez_S = -2\frac{U_0}{E}\,. \tag{B.9}$$

The last equation, (B.9), is the one that determines the spectrum. The "barrier" regime of parameters is when $U_o \gg E$; on the other hand, if $U_0 \ll E$, the mode wavefunctions will not feel the presence of the δ function potential appreciably. Let us therefore concentrate on the barrier regime $U_0 \gg E$. Then the eigenvalues of E will be those for which either $\cot Ez_A$ is large and negative (we call these the A side modes) or where $\cot Ez_S$ is large and negative (these modes will be called the SM side modes). We do not consider the case where the well lengths are tuned and both cot terms become large at the same time.

Let us first look at the A side modes. We have $\cot Ez_A \approx -2U_0/E \gg 1$ so $\sin Ez_A \approx -E/(2U_0)$ while $\cos Ez_S \sim 1$. Then the continuity condition (B.5) implies

$$N_E^S \sim N_E^A \frac{E}{2U_0}\,. \tag{B.10}$$

We then find that the probabilities P_E^A and P_E^S of finding the particle on the I and SM side, respectively, obey

$$\begin{aligned}\frac{P_E^S}{P_E^A} &\equiv \frac{(N_E^S)^2 z_S}{(N_E^A)^2 z_A}\\ &\sim \frac{z_S}{z_A}\left(\frac{E}{2U_0}\right)^2\,.\end{aligned} \tag{B.11}$$

We remind the reader that the corresponding expression in the two throat RS setup was

$$\frac{P_E^S}{P_E^A} \sim \frac{z_S}{z_A}\left(\frac{m}{k}\right)^4\,. \tag{B.12}$$

The two formulae seem to be very different; in particular, the powers of E and m (which are analogs of each other) differ.

This discrepancy brings us to a question we should have answered right in the beginning: how do we compare the two setups, or, more precisely, what parameter values in the square well model should give results comparable to a given set of parameters in the two throat RS setup? A naive guess might be that the integral of the potential in both cases should be comparable; however, there is no good argument saying that the integral of the potential is a physically meaningful quantity.[13] Hence we propose to set the model parameters such that

[13] In fact, if one considers a slowly varying potential W, one can approximate the wavefunction as $\exp[\sqrt{W-E^2}z]$, so the relevant quantity describing the suppression of a wave function by the barrier would appear to be $\exp[\int dz\sqrt{W-E^2}]$, *i.e.,* the integral of the square root of the potential. Such an integral does not make sense for the δ function potential we are considering; of course, the approximation of a slowly varying potential is obviously invalid as well.

the tunnelling rate of plane waves (which is a mathematically well-defined and physically meaningful quantity) are the same for the two barriers.

In fact, the tunnelling rate P_{RS} of the doubled RS model is known and is given precisely by the factor $(m/k)^4$ entering (B.12). Let us therefore calculate the tunnelling rate for the δ-function barrier. We are considering plane waves and hence effectively infinite z_A and z_S; the problem now has a continuous spectrum. For the tunnelling calculation we simply require the wavefunction on the incoming (A) side to be a combination of the incoming and reflected plane wave,

$$\psi^A = Ae^{iEz} + Be^{-iEz}\,, \tag{B.13}$$

while on the outgoing (SM) side the wavefunction should have just the transmitted component,

$$\psi^S = Ce^{iEz} \tag{B.14}$$

Continuity at $z = 0$ implies

$$A + B = C \tag{B.15}$$

while the first derivative jump condition leads to

$$iE\frac{C-(A-B)}{C} = 2U_0\,. \tag{B.16}$$

Extracting the tunnelling rate $P_{sq} \equiv C^2/A^2$ is simple and the result is

$$P_{sq} = \frac{E^2}{U_0^2}\,. \tag{B.17}$$

Hence the tunnelling rate P_{sq} is, up to a factor of 4, precisely the factor entering (B.11) (we disregarded such factors in the derivation of (B.11) anyway).

C Decay rates of KK modes

We present an effective 4-dimensional calculation of the decay rates of KK modes into two particles that can be either gravitons or lower lying KK modes (or one of each). The effective 4-dimensional 3-point couplings ζ for these processes are calculated in the main text. The calculation we do here is in principle a standard textbook one with the added complication of having a tower of KK modes accessible as decay products.

The effective 4-dimensional interaction is

$$S_{int} = \int d^4x\zeta\phi_0(x)\phi_1(x)\phi_2(x) \tag{C.1}$$

where we take ϕ_0 to be the decaying mode with mass m_0 and ϕ_1, ϕ_2 are the products with masses m_1, m_2 (which need not be nonzero). Note that the coupling "constant" ζ can depend on the momenta of the particles. Since the decaying mode is massive, we can go into its rest frame. Let us denote the particles' energies by $\omega_0 = m_0, \omega_1, \omega_2$ and their space momenta by $\vec{p}_0 = 0, \vec{p}_1, \vec{p}_2$. The decay amplitude is simply ζ and the decay rate Γ_{m_1,m_2} is (we omit all factors of 2π)

$$\Gamma_{m_1,m_2} \sim \int d^3p_1 d^3p_2 \delta^3(\vec{p}_1 + \vec{p}_2)\delta(m_0 - \omega_1 - \omega_2)\frac{\zeta^2}{m_0\omega_1\omega_2}\,. \tag{C.2}$$

When comparing the decay rates into KK modes and into gravitons, one must perform a sum over all accessible KK modes to obtain the total decay rate Γ_{KK} into KK modes,

$$\begin{aligned}\Gamma_{2KK} &= \sum_{m_1+m_2<m} \Gamma_{m_1,m_2} \\ &\approx z_S^2 \int_0^{m_0} dm_1 \int_0^{m-m_1} dm_2 \Gamma_{m_1,m_2}\,,\end{aligned} \tag{C.3}$$

where in the second line we have approximated the sum over a dense discrete spectrum by an integral. If one of the final states is a graviton, there is only one integral (say over m_1):

$$\Gamma_{KK,g} \approx z_S \int_0^{m_0} dm_1 \Gamma_{m_1,m_2=0} \tag{C.4}$$

Evaluating Γ_{m_1,m_2} is simple. The integral over $\vec{p}_2$ is trivial; the energy δ function then forces the magnitude of $\vec{p}_1$ to be

$$\vec{p}_1^{\,2} = \frac{\left(m_0^2 - m_1^2 - m_2^2\right)^2 - 4m_1^2 m_2^2}{4m_0^2} \,. \tag{C.5}$$

Taking account of the δ function then gives

$$\Gamma_{m_1,m_2} \sim \frac{|\vec{p}_1|\zeta^2}{m_0^2} \tag{C.6}$$

where ζ, if it depends on the momenta, is evaluated with $\vec{p}_1 = -\vec{p}_2$ given by (C.5) (by rotational invariance ζ cannot depend on the direction of $\vec{p}_1$). The two main cases of interest in Section 4 are when ζ is independent of momenta and when it contains a factor of $p_0 \cdot p_1 = m_0\sqrt{m_1^2 + p_1^2}$. (One could also contemplate $p_1 \cdot p_2$; this coupling should be comparable to $p_0 \cdot p_1$.) Let us treat both cases together by writing ζ as

$$\zeta = \widetilde{\zeta}(p_0 \cdot p_1)^\beta \tag{C.7}$$

with $\beta = 0, 1$. We can then write

$$\begin{aligned} \Gamma_{2KK} &\sim z_S^2 \int_0^{m_0} dm_1 \int_0^{m-m_1} dm_2 \widetilde{\zeta}^2 m_0^{2\beta-2} (m_1^2 + \vec{p}_1^{\,2})^\beta \\ &\sim z_S^2 m_0^{4\beta} \widetilde{\zeta}^2 \int_0^1 dv_1 \int_0^{v_1} dv_2 w_1 \left(v_1^2 + w_1 (v_1, v_2)^2\right)^\beta \,, \end{aligned} \tag{C.8}$$

where we have denoted

$$w_1^2 = \frac{\vec{p}_1^{\,2}}{m_0^2} = \frac{\left(1 - v_1^2 - v_2^2\right)^2 - 4v_1^2 v_2^2}{4} \tag{C.9}$$

i.e., the momentum $\vec{p}_1^{\,2}$ in units of m_0^2. The phase space integral is now written as a dimensionless integral that will simply give a number that we expect to not differ significantly from 1; we duly disregard it and obtain

$$\Gamma_{2KK} \sim z_S^2 m_0^{4\beta+1} \widetilde{\zeta}^2 \,. \tag{C.10}$$

The total decay rate into one graviton and one KK mode can be treated similarly; the result is simply one less factor of $z_S m_0$ because of the missing integration over m_2:

$$\Gamma_{KK,g} \sim z_S m_0^{4\beta} \widetilde{\zeta}^2 \,. \tag{C.11}$$

D Inclusion of a sink in a two-well system

In this Appendix we discuss two-well systems in which the wavefunction decays with rates that are different on each side of the barrier. We will first gather basic facts for a single well.

D.1 A potential well with a sink

Let us consider quantum mechanics of a square infinite well of length z_0 that has a constant imaginary term in the potential. We write the wavefunction as $\Psi(z,t) = T(t)\psi(z)$ with $T(t) = \exp(i\omega t)$ and allow ω to be complex. The Schrödinger equation for ψ is then

$$\left[-\frac{1}{2}\frac{\partial^2+}{\partial i^2}S_0\right]\psi = \frac{1}{2}\omega^2\psi\,, \tag{D.1}$$

and the boundary conditions are the standard

$$\psi(z=0) = \psi(z=L) = 0\,. \tag{D.2}$$

The solution is

$$\psi(z) = N\sin\lambda z \tag{D.3}$$

where

$$\lambda = \sqrt{\omega^2 - 2iS_0} = \frac{n\pi}{L}\,. \tag{D.4}$$

We hence find that unlike in the usual case, the wavenumber λ and the frequency differ and while the wavenumber is real (this is dictated by the boundary conditions), the frequency is complex,

$$\omega_n = \sqrt{\frac{n^2\pi^2}{L^2} + 2iS_0}\,, \tag{D.5}$$

and the wavefunction can either decay or grow exponentially depending on which branch of the square root one takes. Of course, if the iS_0 term is supposed to represent a sink, one must choose the sign for which the wavefunction decays.

D.2 δ-function barrier with a sink

Let us now consider the toy model of a δ-function potential barrier, where we add a sink term that has a different magnitude on each side of the barrier, $S = S^A = \text{const}$ for $z < 0$ and $S = S^S = \text{const}$ for $z > 0$. We again write the full time-dependent wavefunction as $\Psi(z,t) = T(t)\psi(z)$ with $T(t) = \exp(i\omega t)$, where ω is in general complex and is the same on both sides. The boundary conditions $\psi(z = -z_A) = \psi(z = z_S) = 0$ together with the Schrödinger equation (D.1) (with the appropriate sink on each side) imply

$$\begin{aligned} \psi(z) &= N^A \sin\lambda^A(z + z_A)\,, \qquad z < 0 \\ \psi(z) &= N^S \sin\lambda^S(z - z_S)\,, \qquad z > 0 \end{aligned} \tag{D.6}$$

with the wavenumbers given in terms of ω as

$$\lambda^{A,S} = \sqrt{\omega^2 - 2iS^{A,S}}\,. \tag{D.7}$$

The matching conditions at $z = 0$ are exactly the same as in the sink-less case discussed in Appendix B and can be written as

$$N^A \sin\lambda^A z_A = -N^S \sin\lambda^S z_S\,, \tag{D.8}$$

$$\lambda^A \cot\lambda^A z_A + \lambda^S \cot\lambda^S z_S = -2U_0\,. \tag{D.9}$$

Let us again assume we are in the "barrier" regime $U_0 \gg 1/z_A > 1/z_S$. To satisfy (D.9), one of the cot functions must be large (we assume the wells are not tuned, so at most one of the cot's can be large for any value of ω).

As a function of a complex variable x, $\cot x$ is large only near $x_n = n\pi$. Let us assume that it is the A side cot that is large, so we find that the A side modes will have wave numbers

$$\lambda_n^A \approx \frac{n\pi}{z_A}\,. \tag{D.10}$$

In this case the corresponding λ^S will be complex,

$$\lambda_n^S \approx \sqrt{\frac{n^2\pi^2}{z_A^2} - 2i(S^S - S^A)}\,. \tag{D.11}$$

The presence of a complex term in the jump condition (D.9) implies that λ_n^A will also have a small imaginary part and hence that even if $S^A = 0$, the wavefunction of an A mode will slowly decay via "seepage" and subsequent decay on the SM side. The imaginary part of λ_n^A can be estimated as

$$\text{Im }\lambda_n^A \sim \frac{n}{U_0^2 z_A^2} \times \begin{cases} z_S(S^A - S^S) & \text{for } |S^S - S^A| \ll \frac{n}{z_A z_S} \\ \frac{n}{z_A} & \text{for } \frac{n}{z_A z_S} \lesssim |S^S - S^A| < \frac{n^2}{z_A^2} \\ \sqrt{S^S - S_A} & \text{for } |S^S - S^A| \gtrsim \frac{n^2}{z_A^2}\,. \end{cases} \tag{D.12}$$

so even for large S^S it is suppressed by $1/(U_0 z_A)^2$, which for low-lying modes ($n \sim 1$) roughly equals the tunnelling probability P_{sq} given in (B.17).

Let us now look at the case when the sink is only turned on the SM side, *i.e.,* $S^A = 0$, while $S^S \neq 0$ and comparable to $1/z_A^2$. While λ_n^A is (nearly) real, $\lambda_n^S = a + ib$ has a sizable imaginary part; this means that the wavefunction on the SM side,

$$\psi(z) = \sin \lambda^S (z - z_S) \tag{D.13}$$

will actually be largest near $z = 0$ and will decrease in magnitude roughly as $\exp b(z - z_S)$. This is what one would expect intuitively: the wavefunction has roughly constant magnitude on the A side; on the SM side very close to the barrier the magnitude will be determined by continuity (D.8) and so will be not affected by the sink very much, but further away from the barrier the wavefunction decays roughly exponentially (actually as a sum of a cosh and sinh term) due to the presence of the sink. As a consequence, the wavefunction remains normalizable to 1 even in the limit $z_S \to \infty$ (while keeping z_A constant), rather then becoming plane wave normalizable as in the case without a sink: continuity (D.8) implies

$$\begin{aligned} |N^S|^2 &= |N^A|^2 \sin \lambda^A z_A|^2 \frac{1}{|\sin(a+ib)z_S|^2} \\ &\approx |N^A|^2 |\sin \lambda^A z_A|^2 \frac{1}{\cosh 2bz_S}\,, \end{aligned} \tag{D.14}$$

while the normalization integral on the SM side is

$$\begin{aligned} I^S &= \int_0^{z_S} dz |\sin(a+ib)(z - z_S)|^2 \\ &= \int_0^{z_S} dz \,[\cosh 2b(z - z_S) + \cos 2a(z - z_S)] \\ &\approx \frac{1}{2b} \sinh 2bz_S \end{aligned} \tag{D.15}$$

so the product $|N^S|^2 I^S$ remains finite for $z_S \to \infty$. Effectively the particle penetrates the SM side only to distance $z \sim 1/b$ (that penetration is of course suppressed by the usual tunnelling probability – the factor $\sin \lambda^A z_A$ is small). The magnitude of b depends of course on S^S; we remind the reader that $a + ib \equiv \lambda^S \approx \sqrt{\frac{n^2\pi^2}{z_A^2} - 2iS^S}$.

E Sinks and reduced decay rates

In this Appendix we derive the values of the sinks S^A, S^S in a two-throat RS system that reproduce given decay rates Γ^A, Γ^S. The sinks are an effective description of the decay; in particular, they are different for different frequencies. Indeed, if the sinks were frequency-independent, the decay rates for heavy modes with mass $m \gg S$ would be given by $\Gamma \sim S/m$ (where the frequency $\omega = m + i\Gamma$) and hence would decrease with increasing m, contrary to what one expects, and obtains, for the decay of KK modes in our model. Apriori it is not completely clear that the sinks have to be the same for two modes of the same frequency that are localized in different throats; however, if the sinks were different, one runs into potential inconsistencies with some modes simply disappearing from the spectrum when one of the throats changes length, so it appears that the sinks cannot depend on whether the particular mode is localized on one side or the other. In fact, this conclusion can be verified independently by an explicit calculation based on the continuity equation of the probability density; we will not describe the calculation in detail here.

Let us take a particular mass and denote $\delta S \equiv S^A - S^S$; then we have $(\lambda^S)^2 = (\lambda^A)^2 + 2i\delta S$. Given the decay rates Γ^A and Γ^S of a particular mode in the A and SM throats, respectively, we will find useful to define reduced decay rates Γ_0^A, Γ_0^S that only depend on the properties of the particles the mode decays into, while the dependence on the size of the wavefunction of the decaying mode as well as on the length of the throat is scaled out:

$$\begin{aligned} \Gamma^A &= \Gamma_0^A \left|(N^A)^2 \left(1 + (Q^A)^2\right)\right|^2 z_A \,, \\ \Gamma^S &= \Gamma_0^S \left|(N^S)^2 \left(1 + (Q^S)^2\right)\right|^2 z_S \,. \end{aligned}$$

For example, for an A throat mode $|(N^A)^2[1 + (Q^A)^2]|z_A \sim 1$, so $\Gamma^A \sim \Gamma_0^A$, but $|(N^S)^2[1 + (Q^S)^2]|z_S \sim \sigma_A^5/\sigma^S$ and hence $\Gamma^S \sim \Gamma_0^S |\lambda/k|^4 z_S/z_A$. In other words, the reduced decay rates encode properties of the throat and modes into which the decaying mode decays into. Regarding the two-throat system as two weakly coupled single-throat systems leads us to expect that the reduced decay rates should determine, up to small corrections, the corresponding sinks (and the corrections should vanish in the limit of an infinite barrier).

Let us start by considering an A throat KK mode. The aim will be to find the imaginary part of its wavenumbers induced by the presence of a barrier and a particular set of sinks; this will allow us to express the (known) decay rate of the mode in terms of the two (unknown sinks). Repeating the same procedure for an SM throat mode of the same mass (that has a different decay rate but the same sinks) gives us the second equation for the sinks; this system can be then solved to find the sinks. We will assume that δS is at least somewhat smaller than m^2, and we will work to lowest non-trivial order in perturbation theory in m/k.

For an A throat KK mode, the matching condition (5.8) implies

$$Q_m^A \approx -\frac{\lambda^S Y_1^S Y_2^S + \lambda^A Y_1^A Y_2^S}{\lambda^A J_1^A Y_2^S} \,, \tag{E.1}$$

where we have denoted $Y_1^S \equiv Y_1(\lambda^S/k)$ etc. Using the small-argument approximations (A.1) we have

$$Q_m^A \approx -\frac{k^2}{(\lambda^A)^2}\left(2 + \frac{2i\delta S}{(\lambda^A)^2}\right) \,, \tag{E.2}$$

so Q_m^A is large. Using the general formula (2.14) and the asymptotic form of the Bessel functions we have

$$Q_m^A \approx \cot(\lambda^A \tilde{z}_A - 3\pi/4) \,; \tag{E.3}$$

$|Q_m^A| \gg 1$ then implies that

$$\begin{aligned} \sin(\lambda^A \tilde{z}_A - 3\pi/4) &\approx \frac{(\lambda^A)^2}{k^2} \frac{1}{2 + \frac{2i\delta S}{(\lambda^A)^2}} \\ &\approx \frac{(\lambda^A)^2}{k^2} \frac{1}{2}\left(1 - \frac{i\delta S}{(\lambda^A)^2}\right) \,. \end{aligned}$$

This in turn implies that

$$\lambda^A \tilde{z}_A - 3\pi/4 \approx n\pi + \frac{(\lambda^A)^2}{k^2}\frac{1}{2}\left(1 - \frac{i\delta S}{(\lambda^A)^2}\right) . \tag{E.4}$$

If the two throats were decoupled, we would have $\lambda^A_{dec}\tilde{z}_A - 3\pi/4 \approx n\pi$; let us denote the imaginary part of λ^A induced by the presence of the SM throat with its sink by $\delta\lambda^A \equiv \mathrm{Im}\,\{\lambda^A - \lambda^A_{dec}\}$. Eq. (E.4) can then be written as

$$\delta\lambda^A \approx -\frac{\delta S}{2k^2\tilde{z}_A} . \tag{E.5}$$

The derivation here used the assumption $\cos(\lambda^A\tilde{z}_A - 3\pi/4) \approx 1$; this is true whenever the imaginary part of $\lambda^A\tilde{z}_A$ is small. Under our assumptions we indeed have $\delta\lambda^A\tilde{z}_A \ll 1$, so the calculation is consistent.

The imaginary part of the wavenumber determines the decay rate Γ_A of the mode via (recall that $(m + i\Gamma_A/2)^2 = \omega^2 = (\lambda^A)^2 + 2iS^A$)

$$\Gamma_A \approx 2\delta\lambda^A + \frac{2S^A}{m} . \tag{E.6}$$

In general, the decay rate of the (A throat) mode Γ_A is the sum of the decay rate Γ^A_A in the A throat and the decay rate Γ^S_A in the the SM throat, $\Gamma_A = \Gamma^A_A + \Gamma^S_A$. We would like to express these partial decay rates through the corresponding reduced decay rates (E.1). For that we note that for an A throat KK mode, we have $|N^A|^2 z_A \sim 1$ and $|N^S|^2 z_S \sim P_{RS} z_S/z_A$, where the tunnelling probability $P_{RS} \sim m^4/k^4$. We therefore have

$$\Gamma_A \sim \Gamma^A_0 + \Gamma^S_0 P_{RS}\frac{z_S}{z_A} , \tag{E.7}$$

which, together with (E.6), implies

$$\Gamma^A_0 + \Gamma^S_0 P_{RS}\frac{z_S}{z_A} \sim \delta\lambda^A + \frac{2S^A}{m} . \tag{E.8}$$

Repeating the same argument for an SM throat KK mode leads to an analogous equation,

$$\Gamma^S_0 + \Gamma^A_0 P_{RS}\frac{z_A}{z_S} \sim \delta\lambda^S + \frac{2S^S}{m} . \tag{E.9}$$

Here $\delta\lambda^S$ is given by an expression analogous to (E.5), namely

$$\delta\lambda^S \approx \frac{\delta S}{2k^2\tilde{z}_S} . \tag{E.10}$$

We now have two equations, (E.8) and (E.9), for the two unknown sinks. (Note that while we have written the equations up to order one factors, one could write them exactly, though in a much more cluttered and less intuitive form.) The solution can be written as

$$\begin{aligned} S^A + S^S &\sim \frac{m}{2}\left[\Gamma^A_0\left(1 + P_{RS}\frac{z_A}{z_S}\right) + \Gamma^S_0\left(1 + P_{RS}\frac{z_S}{z_A}\right)\right] , \\ S^A - S^S &\sim \frac{m}{2}\frac{1}{1 + \frac{m(z_S - z_A)}{4k^2 z_S z_A}}\left[\Gamma^A_0\left(1 - P_{RS}\frac{z_A}{z_S}\right) - \Gamma^S_0\left(1 - P_{RS}\frac{z_S}{z_A}\right)\right] . \end{aligned} \tag{E.11}$$

Clearly, for a large enough barrier height k/m (such that the factors $P_{RS}z_S/z_A$ and $m(z_S - z_A)/(4k^2 z_S z_A)$ are both small), we find $S^A \sim \Gamma^A_0 m/2$, $S^S \sim \Gamma^S_0 m/2$ as expected; the presence of the finite barrier induces corrections suppressed by various powers of the barrier factor.

References

[1] S. B. Giddings, S. Kachru and J. Polchinski, "Hierarchies from fluxes in string compactifications," Phys. Rev. D **66**, 106006 (2002) [arXiv:hep-th/0105097].

[2] L. Randall and R. Sundrum, "A large mass hierarchy from a small extra dimension," Phys. Rev. Lett. **83**, 3370 (1999) [arXiv:hep-ph/9905221].

[3] H. L. Verlinde, "Holography and compactification," Nucl. Phys. B **580**, 264 (2000) [arXiv:hep-th/9906182].

[4] G. R. Dvali and S. H. H. Tye, "Brane inflation," Phys. Lett. B **450**, 72 (1999) [arXiv:hep-ph/9812483].

[5] X. g. Chen, "Multi-throat brane inflation," Phys. Rev. D **71**, 063506 (2005) [arXiv:hep-th/0408084].

[6] S. Kachru, R. Kallosh, A. Linde, J. Maldacena, L. McAllister and S. P. Trivedi, "Towards inflation in string theory," JCAP **0310**, 013 (2003) [arXiv:hep-th/0308055].

[7] N. Lambert, H. Liu and J. Maldacena, "Closed strings from decaying D-branes," arXiv:hep-th/0303139.

[8] D. Chialva, G. Shiu and B. Underwood, "Warped reheating in multi-throat brane inflation," JHEP **0601**, 014 (2006) [arXiv:hep-th/0508229].

[9] N. Barnaby, C. P. Burgess and J. M. Cline, "Warped reheating in brane-antibrane inflation," JCAP **0504**, 007 (2005) [arXiv:hep-th/0412040].

[10] L. Kofman and P. Yi, "Reheating the universe after string theory inflation," Phys. Rev. D **72**, 106001 (2005) [arXiv:hep-th/0507257].

[11] A. R. Frey, A. Mazumdar and R. Myers, "Stringy effects during inflation and reheating," Phys. Rev. D **73**, 026003 (2006) [arXiv:hep-th/0508139].

[12] H. Firouzjahi and S. H. Tye, "The shape of gravity in a warped deformed conifold," JHEP **0601**, 136 (2006) [arXiv:hep-th/0512076].

[13] X. Chen and S. H. Tye, "Heating in Brane Inflation and Hidden Dark Matter," arXiv:hep-th/0602136.

[14] S. Dimopoulos, S. Kachru, N. Kaloper, A. E. Lawrence and E. Silverstein, "Generating small numbers by tunneling in multi-throat compactifications," Int. J. Mod. Phys. A **19**, 2657 (2004) [arXiv:hep-th/0106128].

[15] J. Lykken, R. C. Myers and J. Wang, "Gravity in a box," JHEP **0009**, 009 (2000) [arXiv:hep-th/0006191].

[16] I. R. Klebanov and M. J. Strassler, "Supergravity and a confining gauge theory: Duality cascades and χSB-resolution of naked singularities," JHEP **0008**, 052 (2000) [arXiv:hep-th/0007191].

[17] I. R. Klebanov and A. A. Tseytlin, "Gravity duals of supersymmetric SU(N) x SU(N+M) gauge theories," Nucl. Phys. B **578**, 123 (2000) [arXiv:hep-th/0002159].

[18] I. Oda, "Mass hierarchy from many domain walls," Phys. Lett. B **480**, 305 (2000) [arXiv:hep-th/9908104].

[19] H. Hatanaka, M. Sakamoto, M. Tachibana and K. Takenaga, "Many-brane extension of the Randall–Sundrum solution," Prog. Theor. Phys. **102** (1999) 1213 [arXiv:hep-th/9909076].